BIOLOGICAL AND CHEMICAL SYNTHESIS OF Fe_3O_4 NANOPARTICLES AND EVALUATION OF IT'S ANTIBACTERIAL ACTIVITY

By: MEKO DUBE

A THESIS SUBMITTED TO DEPARTMENT OF

APPLIED CHEMISTRY

SCHOOL OF APPLIED NATURAL SCIENCE

IN PARTIAL FULFILLMENT OF THE REQUIREMENTS FOR THE DEGREE OF MASTER OF SCIENCE IN CHEMISTRY (PHYSICAL STREAM)

OFFICE OF GRADUATE STUDIES

ADAMA SCIENCE AND TECHNOLOGY UNIVERSITY

AUGUST, 2019

ADAMA, ETHIOPIA

BIOLOGICAL AND CHEMICAL SYNTHESIS OF Fe_3O_4 NANOPARTICLES AND EVALUATION OF IT'S ANTIBACTERIAL ACTIVITY

By:

MEKO DUBE

MAJOR ADVISER: BEDASA ABDISA (PhD)

CO – ADVISER: FEDLU KEDIR (PhD)

A THESIS SUBMITTED TO DEPARTMENT OF APPLIED CHEMISTRY

SCHOOL OF APPLIED NATURAL SCIENCE

IN PARTIAL FULFILLMENT OF THE REQUIREMENTS FOR THE DEGREE OF MASTER OF SCIENCE IN CHEMISTRY (PHYSICAL STREAM)

OFFICE OF GRADUATE STUDIES

ADAMA SCIENCE AND TECHNOLOGY UNIVERSITY

AUGUST, 2019

ADAMA, ETHIOPIA

APPROVAL SHEET

Submitted by

_____	_____	_____
Name	Signature	Date

As a thesis research advisors, We hereby certify that we have read and evaluated this thesis prepared under our guidance by Meko Dube. We recommended the paper to be submitted as fulfilling the requirements for the Degree of Master of Science in Chemistry (Physical Chemistry).

_____	_____	_____
Advisor	Signature	Date
_____	_____	_____
Co-advisor	Signature	Date

We the undersigned, members of the boards of examiners of the final open defence by Meko Dube, have read and evaluated her thesis entitled "Biological and Chemical Synthesis of Fe_3O_4 Nanoparticles and evaluation of It's Antibacterial Activity" and examined the candidate. This is, therefore, to certify her thesis work and has been accepted in partial fulfillment of the requirments of the degere of Master of Science in chemistry (Physical Chemistry) complies with the regulation of the Unversity.

_____	_____	_____
Internal Examiner	Signature	Date
_____	_____	_____
External Examiner	Signature	Date
_____	_____	_____
Chair Person	Signature	Date
_____	_____	_____
Department Head	Signature	Date
_____	_____	_____
School Dean	Signature	Date

DECLARATION

I hereby declare that this M.Sc thesis is my original work and has not been presented for a degere in any other university and all source of material used for this thesis have been duly acknowledged.

Name : Meko Dube Signature _____

This MS.c thesis has been submitted for examination with our approval as thesis advisors

Advisor: Bedasa Abdisa (PhD) Signature _____

Co-Advisor: Fedlu Kedir (PhD) Signature _____

Date of Submission _____

DEDICATION

This M.Sc thesis is dedicated to my beloved families whose advice, support and love helped me all along the right way and made me who I am today.

ACKNOWLEDGMENT

First of all I would like to thank Allah, all praise to Allah for all his blessing in the completion of this thesis.

Next and foremost, I would like to express my deep gratitude to my advisor, Dr. Bedasa Abdisa for his kind approach, invaluable suggestions, constructive comments and guidance throughout my thesis work.

Although I would like to express my genuine heartfelt gratitude to my Co-adviser Dr. Fedlu Kedir for his invaluable suggestion, comments, corrections, professional & technical guidance throughout my work for the successful accomplishment of this thesis.

I would like to express my gratitude to Biology lab technicians and Material Engineering lab technicians for their good help and generating experimental data during my work.

Finally, I would like to acknowledge Department of Applied Chemistry for facilitating all adminstrative and academic issues for the success of my study during my stay in the University.

Table of Contents

LIST OF TABLES

Tables Pages

LIST OF FIGURES

Figures pages

ABSTRACT

Iron oxide is interesting because it has vast applications in various areas. In this study iron oxide (Fe_3O_4) nanoparticles were synthesized by green method using 1:2 ratios of ferrous sulphate hepta hydrate and ferric chloride hexahydrate as precursory with the presence of hagenia abyssinica flower extract in different ratio and chemical method by using ferric nitrate and ethylene glycol. The synthesized Fe_3O_4 nanoparticles were characterized by x-ray diffraction (XRD), scanning electron microscopy-energy dispersive x-ray spectroscopy (SEM-EDS), ultraviolet visible spectroscopy (UV-Vis) and Fourier transformer infrared spectroscopy (FTIR). The crystal structure of nanoparticles were determined by XRD analysis and the particle size of the nanoparticles were in the range of 8 – 9.2 nm for green synthesized nanoparticles and 9.28nm for that of chemically synthesized nanoparticles.The shape of the nanoparticles and elemental composition were determined by SEM-EDS respectively. The UV-Vis investigation confirms the formation of iron oxide NPs i.e. the reflectance peak was exist at 324.4 nm for green synthesized nanoparticles and 328.5 nm for chemically synthesized nanoparticles. Fourier transformer infrared spectroscopy study confirmed the presence of amines, carboxylic acids, phenols and alcohols . The synthesized nanoparticles were tested for anti bacterial activity. The chemically synthesized Fe_3O_4 Nanoparticle showed a good antibacterial activity on E. coli and S. aureus bacterial strains.

Key words: - Fe_3O_4 Nanoparticles, Green Synthesis, Chemical Syntheis, Antibacterial Activity.

1. INTRODUCTION

1.1. Background of the Study

Nanotechnology can be defined as the manipulation of matter through certain chemical and physical processes to create materials with specific properties, which can be used in particular applications. A nanoparticle can be defined as a microscopic particle that has at least one dimension less than 100 nanometers in size (Thakkar *et al*., 2010). In principle any collection of atoms bonded together with a structural radius of less than 100 nm can be considered as a nanoparticle. The key factors of nanoparticles are small particle size, narrow size distribution, low agglomeration and high dispersion. They are a link between bulk materials and atomic or molecular structures. Nanoparticles have different chemical and physical properties than bulk materials such as lower melting points, higher surface area, mechanical strength, specific optical properties and specific magnetizations (Horikoshi and Serpone, 2014). Nanomaterials can be synthesized by different methods including chemical, physical, and biological methods. Biosynthesis of nanoparticles could be an alternative to traditional chemical methods for the production of metallic nanomaterials in a clean, nontoxic and ecologically sound manner (Ahmad *et al*., 2011).

Moreover, in green synthesis processes there is no need to use high pressure, energy, temperature and toxic chemicals. Plant-mediated biological synthesis of nanoparticles has gained importance only in the recent years. Synthesis of nanoparticles using plants provides more biocompatible nanoparticles than chemical synthesis, whereas chemical synthesis may lead to the presence of some toxic chemical species on the surface of the nanoparticles that may have undesirable effects in biomedical applications. Plant extracts reduce the metal ions in a shorter time as compared to microbes. Depending upon plant type and concentration of phytochemicals, nanoparticles are synthesized within a few minutes or hours (Rai *et al*., 2008). Nanomaterials can be applied in various fields such as cosmetics, paints, displays, batteries, medicine, catalysis, gas sensor, food engineering (production, processing, safety and packaging), agriculture, energy (storage and conversion) and construction (Arivalagan *et al*., 2011). Nanotechnology has also entered into

action to address the underlying problem in microbiology and the counteracting of antibiotic resistant microorganisms (Eiglesias *et al*., 2007).

Iron oxide (Fe_3O_4) nanoparticles have attracted much interest because they belong to the class of materials having non-toxicity and biological compatibility due to the presence of Fe (II/III) ions (Kandpal *et al*., 2014).

In the past decade, the synthesis of iron oxide (Fe_3O_4) nanoparticles has been intensively developed not only for its fundamental scientific interest but also for many technological and biomedical applications (Laurent *et al*., 2008). Fe_3O_4 nanoparticles have a high specific surface area, so they are able to interact with bacterial surface structures. Furthermore, because of their relatively small size, they can facilitate the particle uptake by bacterial cells. The Fe_3O_4 nanoparticles are produced through various physicochemical methods (Glasgow *et al*., 2016). The chemical approaches may be harmful for humans and impose environmental and health risks. In another approach, magnetic nanoparticles are produced by biological resources (biosynthesis or green synthesis).

Here, the aim of this project work was to evaluate and compare the antibacterial activity of Fe_3O_4 nanoparticles synthesised both by the chemical and green methods on a common bacterial strain in clinical practice (Khorrami *et al*., 2018).

1.2. Statement of the Problem

Bacterial infections are major contributors to morbidity and have become increasingly difficult to manage due to the emergence of antimicrobial resistance. The prevalence of antibiotic resistance and multi drug resistant strains Gram +ve and Gram −ve microbes a serious threat to global population. Such resistance is due to indiscriminate use of antibiotics favoring evolution of novel antibiotic resistance strains at faster pace (Raghunath & Perumal, 2017). The World Health Organization (WHO) highlighted one of the most common causes of death in the world due to microbial contamination and pathogens resistance to drugs (Sportelli *et al*., 2016*)*.Therefore synthesis of new and effective antimicrobial agents seems to be of greater importance. Recent advances in the field of nanotechnology bolster the ability to prepare metal oxide nano particles (NPs) of specific size and shape which contribute to the development of new antibacterial agents.

Therefore, Fe_3O_4 nanoparticles are attracting much attention in the field of biomedicines either as contrast agents for magnetic resonance imaging, heating mediators for hyperthermia, drug/gene delivery carriers and antimicrobial agents (Azam *et al*., 2012).

NPs have shown broad-spectrum antibacterial activities against Gram $_+$ve and Gram $_-$ve bacteria because metal NPs have the ability to change the metabolic activity of bacteria (Chatzimitakos and Stalikas, 2016).

1.3. Objective of the Study

1.3.1. General objective

The general objective of this study was to synthesize Fe_3O_4 nanoparticles using chemical method and green method using 'Kosso'*hagenia abyssinica* plant flower extract and to study their antibacterial activity against *Staphylococcus aureus* and *Escherichia coli*.

1.3.2. Specific objectives

The specific objectives were

- ✓ To synthesize Fe_3O_4 nanoparticles by solgel method from iron salt precursors
- ✓ To synthesize Fe_3O_4 nanoparticles using aqueous extract of 'Kosso' *Hagenia abyssinica* plant and iron salt precursors.
- ✓ To characterize the synthesized Fe_3O_4 nanoparticle using techniques such as UV-Visible, FT-IR, XRD and SEM-EDX.
- ✓ To evaluate potential of Fe_3O_4 nanoparticle against *Staphylococcus aureus* and *Escherichia coli*.
- ✓ To compare the antibacterial activity of Fe_3O_4 nanoparticles synthesized by biological and chemical methods.

1.4. Significance of the Study

This study highlights the significance of chemical and green synthesis approaches and the role of biocompatible Fe_3O_4 nanomaterials in technological and economically feasible process and in green method practices of *H.abyssinica*. It also summarizes the quest for sustainable synthesis

process of Fe_3O_4 NPs using *H. abyssinica* for their application to the field of antimicrobial activity like antibacterial activity. From the outcome of those study, new coming researcher were benefited. This research opens up door for further researches on the use of *H. abyssinica* and chemically synthesized in the area.

1.5. Scope of the Study

Synthesis of the nanoparticles were limitted to chemical (solgel) method and biosynthesis technique using 'Kosso' *Hagenia abyssinica* flowers and the characterization of these nanoparticles was also limited to UV-Visible, FT-IR, XRD and SEM techniques. Evaluation of antibacterial activities of the nanoparticles was also limitted to *Staphylococcus aureus* and *Escherichia coli* bacterial stains.

2. LITERATURE REVIEW

Nanotechnology is one of the most important emerging sciences in the 21st century. Research and development in this field has grown rapidly around the world. Nanotechnology has influenced various sciences and has provided many products that have entered the field of biology and medicine, and have had many effects in this regard, including the reduction of the side effects of chemotherapy drugs (Arap *et al.*, 1998).

Nanotechnology has also entered into action to address the underlying problem in microbiology, the counteracting of antibiotic resistant microorganisms. The organic compounds traditionally used for disinfection produce several disadvantages, including toxicity to the human body, and sensitivity to high temperatures and pressures that are present in many industrial processes. For these reasons, the interest in inorganic disinfectants such as metal oxides is increasing (Gordon *et al*., 2011). These inorganic compounds present strong antimicrobial activity at low concentrations. They are also much more stable in extreme conditions considered as non-toxic, and some of them even contain mineral elements essential to the human body. Various nanoparticles of metal oxides have been synthesized and are found a good inhibitor of different bacterial strains. Activity of nanoparticles is directly dependent on the bacterial strain, i.e., gram positive and gram negative bacteria as they have differences in their cell wall (Hajipour *et al*., 2012).

Research in recent years has focused on manufacturing nanomaterials via nanotechnology-based processes that promote the principles of green chemistry and reduce or totally eliminate the use of hazardous chemicals. Thus, ecofriendly green nanotechnology based processes for the manufacture of nanoparticles have attracted considerable interest worldwide (Shah *et al*., 2015). To emphasise this alternative approach, recent research has focused on using biological entities to synthesize a wide variety of nanoparticles. Biosynthesis via unicellular and multicellular biological entities such as actinomycetes, microorganism and plants (Kowshik *et al*., 2003). Offer alternative ecofriendly approaches for producing nanoparticles. Each of these biological entities, to varying degrees, can perform as natural bio factories for producing particular nanoparticles. Each of the biological entities has active molecules and compounds that can act as

reducing agents and stabilizing agents to synthesize nanoparticles with diverse sizes, shapes, compositions, and physicochemical properties (Mohanpuria *et al*., 2008).

2.1. Iron oxides

In the past decade, the synthesis of magnetic IONPs has been intensively developed not only for its fundamental scientific interest but also for its many technological applications, such as targeted drug delivery, magnetic resonance imaging (MRI), magnetic hyperthermia and thermo ablation, bioseparation, and biosensing (Yang, 2008, Lee and Hyeon, 2012, Laurent *et al*., 2011 and Cao *et al*., 2012). Particularly, bioapplications based on magnetic nanoparticles (NPs) have received considerable attention because NPs offer unique advantages over other materials. For example, magnetic IONPs are inexpensive to produce, physically and chemically stable, biocompatible, and environmentally safe (Lu, 2007).

Eight iron oxides are known, among these iron oxides, hematite (α-Fe_2O_3), magnetite (Fe_3O_4) and maghemite (γ-Fe_2O_3) are very promising and popular candidates due to their polymorphism involving temperature-induced phase transition. Each of these three iron oxides has unique biochemical, magnetic, catalytic, and other properties which provide suitability for specific technical and biomedical applications (Cornell and Schwertmann, 2003).

Hematite (α-Fe_2O_3) as the most stable iron oxide and n-type semiconductor under ambient conditions is widely used in catalysts, pigments and gas sensors due to its low cost and high resistance to corrosion. It can also be used as a starting material for the synthesis of magnetite (Fe_3O_4) and maghemite (γ-Fe_2O_3), which have been intensively pursued for both fundamental scientific interests and technological applications in the last few decades (Wu *et al*., 2010). Hematite is an n-type semiconductor with a band gap of 2.3 eV, where the conduction band (CB) is composed of empty d-orbitals of Fe^{3+} and the valence band (VB) consists of occupied 3d crystal field orbitals of Fe^{3+} with some admixture from the O 2p non-bonding orbitals (Zhang *et al*., 1993). As shown in Figure 1(a), Fe^{3+} ions occupy two-thirds of the octahedral sites that are confined by the nearly ideal hexagonal close-packed O lattice.

Maghemite (γ-Fe_2O_3) as shown in Figure 1(b), the structure of γ-Fe_2O_3 is cubic; each unit of maghemite contains 32 O^{2-} ions, 21⅓ Fe^{3+} ions and 2⅓ vacancies. Oxygen anions give rise to a

cubic close-packed array while ferric ions are distributed over tetrahedral sites (eight Fe ions per unit cell) and octahedral sites (the remaining Fe ions and vacancies).Therefore, the maghemite can be considered as fully oxidized magnetite, and it is an n-type semiconductor with a bandgap of 2.0 eV.

Magnetite (Fe_3O_4) as shown in Figure 1(c), Fe_3O_4 has the face centered cubic spinel structure, based on 32 O^{2-} ions and close-packed along the [111] direction. Fe_3O_4 differs from most other iron oxides in that it contains both divalent and trivalent iron. Fe_3O_4 has a cubic inverse spinel structure that consists of a cubic close packed array of oxide ions, where all of the Fe^{2+} ions occupy half of the octahedral sites and the Fe^{3+} are split evenly across the remaining octahedral sites and the tetrahedral sites. In stoichiometric magnetite Fe^{II}/Fe^{III} = 1/2, and the divalent irons may be partly or fully replaced by other divalent ions (Co, Mn, Zn, etc). Thus, Fe_3O_4 can be both an n- and p-type semiconductor. However, Fe_3O_4 has the lowest resistivity among iron oxides due to its small bandgap (0.1 eV) (Boxall *et al*., 1996).

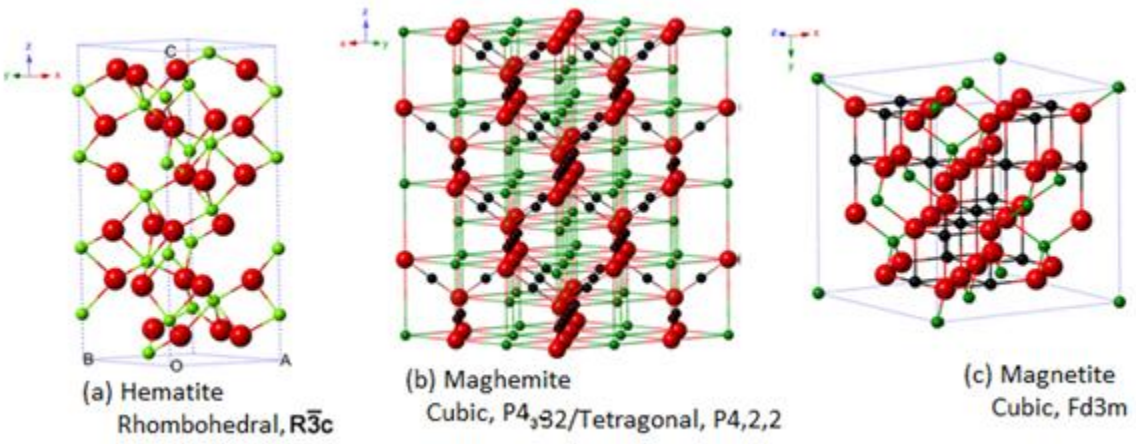

Figure 1. Crystal structure and crystallographic data of the hematite, magnetite and maghemite(the black ball is $Fe^{2+,}$ the green ball is Fe^{3+} and the red ball is O^{2-}(Jiang *et al*., 2015).

2.1.1. Fe_3O_4 nanoparticles

Magnetic nanoparticles possess significant novel phenomena like superparamagnetism, high field irreversibility, high saturation field, extra anisotropy contributions or shifted loops after field cooling. These phenomena are due to the finite size and surface effects that control the

magnetic behaviour of individual nanoparticles. So these groups of nanoparticles have been used in the field of biotechnology, biomedicine, material science, engineering and environmental areas (Tartaj *et al*., 2003). In this context, magnetic nanomaterials, such as iron oxide, magnetite (Fe_3O_4) have been applied in various fields such as drug carriers and contrast agents in magnetic resonance imaging.

Fe_3O_4 nanoparticles have attracted intensive research interest because of their important applications in cancer therapy, drug delivery, magnetic resonance imaging (MRI) and wastewater treatment (Vicky *et al.*, 2010). Because of low cost, availability and properties possessed are similar to that of other metallic nanoparticles and other applications include heat transfer systems as super strong materials, sensors, antimicrobial, bactericidal agents used to coat hospital equipment and also as catalysts.

For this application, certain parameters must be controlled during the synthesis. The control of the size, as well as size distribution, is necessary because it allows the control of the material's properties such as superparamagnetism and hyperthermia. Depending on their size, Fe_3O_4 nanoparticles present different behaviours when an external magnetic field is applied. It is known that abrupt changes in magnetic properties occur when the particle size is reduced from micrometre to the nanometer scale. In nanoscale phenomena of finite size and increase in surface area, effects start to dominate the magnetic behaviour of individual nanoparticles (Figuerola *et al*., 2010).

2.2. Synthesis of Fe_3O_4 Nanoparticles

The manufacture of nanoparticles can be broadly defined into two approaches. The first is the top down approach and involves a material undergoing significant size reduction via physical processes (Birnbaum and Pique, 2011). During size reduction, the resulting particle size, shape, and surface structure are heavily dependent on the technique used. Unfortunately, size reduction also tends to introduce surface imperfections that can significantly impact the overall physicochemical properties of the fabricated nanoparticle.

The second, bottom up approach builds nanoparticles via the assembly of atoms, molecules, and smaller particles or monomers (Cheng *et al*., 2013). There are three main routes for the synthesis

of Fe_3O_4: chemical, physical and biological. These have been investigated in order to produce more stable, soluble, biocompatible, and shape and size-controlled nanoparticles (Jiang *et al*., 2008).

2.2.1. Physical methods of Fe_3O_4 nanoparticles synthesis

In physical methods, nanoparticles are prepared by evaporation-condensation using a tube furnace at atmospheric pressure. Evaporation-condensation and laser ablation are the most important physical approaches. The absence of solvent contamination in the prepared thin films and the uniformity of NPs distribution are the advantages of physical synthesis methods in comparison with chemical processes. Additionally, the advantages of physical methods are speed; radiation is used as reducing agents and no involvement of hazardous chemicals. The disadvantages of physical methods, for example, tube furnace occupies a large space, consumes a great amount of energy while raising the environmental temperature around the source material, and requires a lot of time to achieve thermal stability(Abou *et al*., 2010).

2.2.2. Chemical method of Fe_3O_4 nanoparticles synthesis

Chemical preparation methods are simple, tractable, and efficient, in which the size, composition, and even the shape of the NPs can be managed. Fe_3O_4 can be synthesized through the co precipitation of Fe^{2+} and Fe^{3+} by the addition of a base. The size, shape, and composition Fe_3O_4 NPs synthesized through chemical methods depend on the type of salt used, Fe^{2+} and Fe^{3+}ratio, pH, and ionic strength (Sun *et al*., 2011).

In the last decades, much research has been carried out synthesize Fe_3O_4 NPs, and many reports have described efficient synthesis approaches to produce the shape controlled, stable, biocompatible, and monodispersed iron oxide NPs. The most common methods includes sol-gel techniques (Raja *et al*., 2011). Co-precipitation, thermal decomposition, hydrothermal synthesis, micro emulsion, Sonochemical synthesis and Sonochemical synthetic route have been directed to the synthesis of high quality of iron oxide NPs (Wei *et al*., 2008). However, in all these techniques, aqueous medium is the most efficient pathway to obtain irons magnetic NPs. In this study solgel technique was used to synthesize Fe_3O_4 nanoparticles.

The sol gel process involves formation of an inorganic network of colloidal suspension followed by gelation of the sol solution to form a continuous liquid phase (gel).There are a number of precursors that can serve as sol forming constitutes such as, metal alkoxides, metal organic compounds, salts of inorganic acids, salts of organic acids, etc. In a typical process, precursor solution is dissolved in a solvent. They will undergo hydrolysis and poly condensation processes to form M-O-M bonds. In the hydrolysis process, precursor will hydrolyze and gets hydroxyl group typically through the reaction with water. This sol contains –M–O–M– network with low viscous nature which casts into gel under heating. During gelation, the –M–O–M– network makes a bond with colloidal particles to form a 3D network with high viscosity. The resulting gel is a system consisting of three dimensional network of sol and the solvent. The gel can be further processed to remove the solvent residue. Once the solvent residue is removed, the sol system collapse into an amorphous solid structure, which is known as xerogel (A xerogel is a solid formed from a gel by drying). This material can be sintered in a furnace to transform to a solid crystalline material. Sol-gel processes can be helpful to obtain materials with wide range of oxygen and other metallic compositions such as metal oxide nanoparticles. Sol-gel systems can be controlled to obtain desired particle size, shape and size distributions (Kojima *et al*., 1997).

2.2.3 Green (Biological) method of Fe_3O_4 nanoparticles synthesis

To overcome the shortcomings of chemical methods, biological methods have emerged as viable options. An alternative way of synthesizing metallic nanoparticles is by using living organisms. Biosynthesis is the phenomenon that occurs through biological or enzymatic reactions. The exact mechanism for the synthesis of nanoparticles using biological agents has not yet been perfected, as the different biological agents use a different mechanism with different metals and there are also different bio molecular responses for nanoparticle synthesis (Chokriwal *et al*., 2014).

Nowadays, the biological synthesis is an attractive alternative to traditional methods (physical and chemical approaches) for the production of nanoparticles. The bio-reduction synthesis involves the use of different biological entities, such as, plant extracts, bacteria, fungi, and yeasts. Bio-reduction using plant extracts is the plant extracts containing bioactive alkaloids, phenolic acids, polyphenols, proteins, sugars and terpenoids which confer the ability to reduce metal ions to nanoparticles. The plants are considered an ecological way for nanoparticles

synthesis, especially for those materials which have to be used in the biomedical field (Mittal *et al*., 2013).

Bio-reduction use microorganisms which can survive and grow in high concentrations of toxic metals due to their chemical detoxification potential, as well as their energy dependent efflux in the cell by membrane protein, that functions either as ATP ase or as chemo-osmotic or proton anti-transporter agents. Bio-assisted methods, biosynthesis or green synthesis provides an environmentally benign, low-toxic, cost-effective and efficient protocol to synthesize and fabricate nanoparticles (Saba, 2015).

2.3. Properties of Fe_3O_4 Nanoparticles

Due to their size (diameters ranging from 1 to 100 nm) nanoparticles present specific and controllable properties that are different from those they present on the macroscopic scale thus enabling unique applications(Yetter *et al*., 2009). It is known that the ratio between the number of surface atoms and the number of massive atoms increases significantly with particle size reduction. As the surface atoms have less coordination in relation to massive atoms, nanostructured materials exhibit significantly different physical, chemical, optical, mechanical, electrical and also magnetic properties. The excess of energy of surface atoms contributes for many of the extraordinary characteristics of nanoparticles (Yetter *et al*., 2009). This way, nanoscale materials present great potential for applications in several technological areas such as nano electronics and computer technology, medicine, aeronautics and space exploration, biotechnology and agriculture (Srivastava *et al*., 2009).

2.3.1. Magnetic properties

Magnetic phenomena at the atomic scale were discovered in the early twentieth century, whereas the discovery of the first known magnetic material, Fe_3O_4, revolutionized the field of magnetism. The magnetic properties of a material depend on temperature, the applied magnetic field, and pressure. A change in these variables will result in the existence of two or more forms of magnetism. Ferro- and ferrimagnetic materials like Fe_3O_4 and some of their alloys have particles whose shape is asymmetrical when they are obtained by the grinding of bulk materials. Depending on the procedure used to form particles, they can be crystalline or amorphous

spherical in shape. To a large extent, the synthesis process determines the degree of impurities in a particle, as well as the presence of structural defects, and, hence, the division of these defects inside the particle structure can be used to discover its magnetic properties (Chung *et al*., 2004).

Magnetization depends on the number of unpaired valence electrons present in the atoms of solids and on the relative orientations of the neighboring magnetic moments. Two types of motion of electrons in atoms are responsible for magnetism. One is the spin of electrons around the atom's axis, and the other is the motion of electrons in an orbit around the nucleus (Duan and Guojun, 2005).

2.3.2. Structural properties

Magnetite's crystal structure follows an inverse spinel pattern with alternating octahedral and tetrahedral-octahedra layers (Hill *et al*., 1979). Ferrous species are observed to occupy half of the octahedral lattice sites due to greater ferrous crystal field stabilization energy (CFSE); alternatively, ferric species occupy the other octahedral lattice sites and all tetrahedral lattice sites. Its formula is written as $Fe^{3+}{}_{A}\,[Fe^{3+}Fe^{2+}]_{BO4}$, and in its unit cell, all tetrahedral sites are occupied by Fe^{3+} ("A" sites), and octahedral sites are occupied by Fe^{3+} and Fe^{2+} ("B" sites) (Figure 1A and 1B) (Darbandi *et al*., 2012).

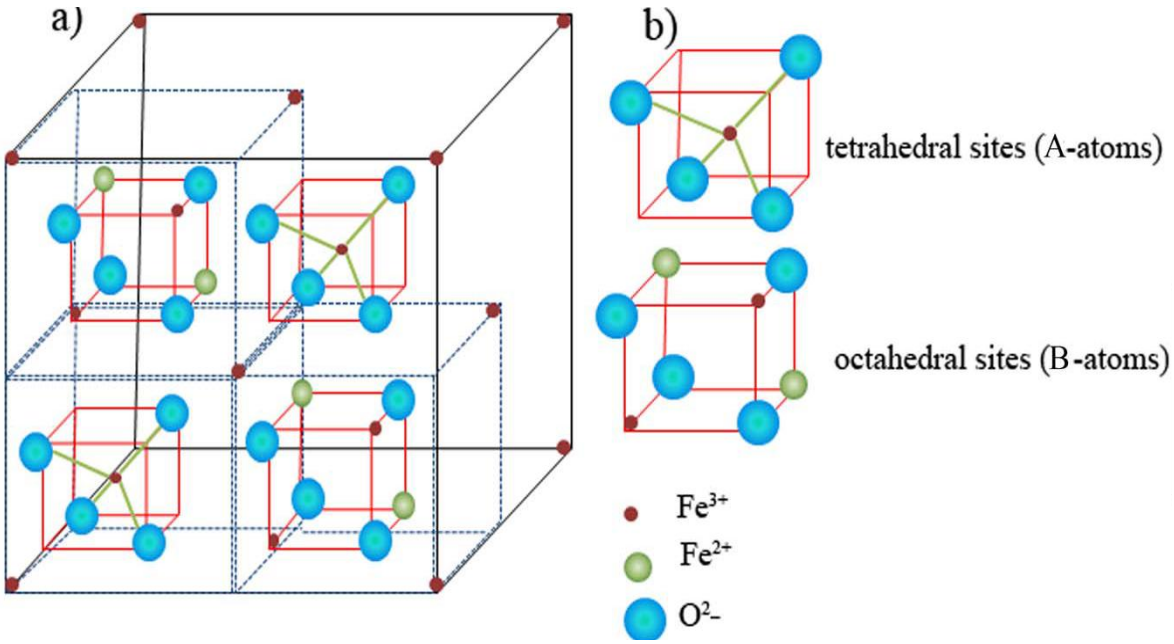

Figure 2. Schematic figures of : (a) simple crystal structure of Fe_3O_4; (b) octahedral and tetrahedral sites showing cations and oxygen

2.3.3. Physical properties

Natural and synthesized magnetite micro-scale crystals exhibit metallic luster and opaque jet black color, Magnetite's density is established at 5.18 g/cm^3, slightly lighter than reddish-brown hematite (α-Fe_2O_3; 5.26 g/cm^3) and somewhat heavier than yellowish orange ferrihydrite (α-FeOOH; 4.26 g/cm^3); pure iron (α-Fe) has a density of 7.87 g/cm^3. At ambient temperatures, magnetite particles exhibit hardness of 5.5 Mohs scale identical to glass. Magnetite particles are not porous. Standard Gibb's free energy of magnetite formation is -1012.6 kJ/ mol; therefore, formation of magnetite is thermodynamically favorable (Cornell and Schwertmann, 1996). Additionally, the standard enthalpy and entropy of magnetite formation are -1115.7 kJ/mol and 146.1 kJ/mol/K, respectively (Hemingway, 1990).

2.3.4. Chemical properties

Fe_3O_4 nanomaterials have great importance because of their magnetic properties and wide applications. The investigation of Fe_3O_4 NPs in biological and material sciences is booming in recent times because of their various chemical and physical properties. They exhibit multiple potential applications, including magnetic fluid, magnetic micro-device, MRI, magnetic

hyperthermia, water purification, and drug delivery. Significant size dependent structural and optical properties of colloidal iron and iron oxide NPs correspond to electrical structure and quantum size effects of NPs. The respective synthesis method can affect their size and crystal structure as well (Estelrich *et al*., 2015).

Chemically, Fe_3O_4 NPs are very active and can easily be oxidized in air, generally resulting in the loss of dispersibility and magnetism. Thus, it is important to keep the stability of magnetic Fe_3O_4 NPs by developing some effective protection strategies and providing proper surface coating (or grafting) with organic molecules, polymers, surfactants, biomolecules, or inorganic layer such as silica, metal, metal sulfide, metal oxide, or nonmetal elementary substances (Wu *et al*., 2009).

2.3.5. Electrical properties

Octahedral sites in the magnetite structure contain ferrous and ferric species. The electrons coordinated with these iron species are thermally delocalized and migrate within the magnetite structure causing high conductivity exchange constants: ranging from -28 J·K to 3 J·K between tetrahedral/octahedral sites and octahedral/octahedral sites, respectively. Magnetite's Verwey transition temperature (118 K) exhibits and ordered arrangement of ferrous and ferric ions on octahedral sites, inhibiting electron delocalization when temperatures fall below Verwey transition temperature. Furthermore, due to electron delocalization effects magnetite can be slightly metal deficient on octahedral sites; such deficiency allows for n- and p-type magnetite semiconductors (Cornell and Schwertmann, 1996).

H. abyssinica is commonly known as Kosso in Ethiopia (Jansen, 1981). The name Kosso is used in several ways in Ethiopia. It can indicate the tree (*Hagenia*), the female inflorescence used for tapeworm (the medicine), the parasite, or in general other taenicidal medicine. *H. abyssinica* is a dioecious tree with distinct male and female trees, both of which are endowed with colourful flowers. The tree attains heights of up to 20 m, with short trunk and thick branches; branchlets are covered by silky brown hairs and ringed with leaf scars. The bark, which can sometimes be very thick in older specimens, is usually brownish in colour, and readily peels in strips. Hairs are quite abundant on young branchlets, petioles and leaves (Negash, 1995).The female flowers of *H. abyssinica* have long been used to expel tapeworm, a very common infestation among

Ethiopians due to the age-long practice of eating raw beef by a large sector of the population. Only female flowers of the Kosso are said to be active as anthelmintics, and they are called 'red Kosso' (Negash, 1995).The first definite crystalline product from Kosso appears to have been the kosin. Bernard *et al*. (1974), in Jansen, 1981 analyzed a sample of Kosso and reported the following composition six organic acids: fumaric acid , α-ketoglutaric acid , succinic acid , citric acid , glycolic acid and malic acid.The following amino acids were identified aspartic acid, threonine, serine, glutaminic acid, proline, glycocol, alanine, valine, cystine, methionine, iso-leucine, leucine, tyrosine, phenylalanine, histidine and arginine (Jansen,1981). This evidences about the medicinal values and phytochemistry of this plant, the present study was used flower extract of *Hagenia abyssinica* for green synthesis of eco-friendly Fe_3O_4 nanoparticles for the study of antibacterial activity against gram negative (*Escherichia coli)* and gram positive bacteria (Staphylococcus aureus). This would also be compared with Fe_3O_4 nanoparticles that was synthesized by chemical method for the same application.

2.4. Application of Fe_3O_4 Nanoparticles

The synthesis of magnetic nanoparticles (MNP) has received great interest in recent years because of new physical and chemical properties of materials at nanoscale. Based on their mesoscopic physical, chemical, thermal and mechanical properties, and in conjunction with control of size, composition and morphology of growth, the synthesis of MNP lead to a wide range of specific technological applications (Teja and Koh, 2009). Among crystal polymorphs of iron (III) known, magnetite (Fe_3O_4) is a promising candidate for its biocompatibility and biodegradable activity. Thus, Fe_3O_4 MNP with crystalline phase corresponding to magnetite appears as an important nanomaterial for various biomedical applications (Pankhurst *et al*., 2003).

2.4.1. Antimicrobial activity of Fe_3O_4 nanoparticles

Antimicrobial agents considerably help to prevent and treat infectious diseases in humans and animals; however, the increase of resistant microbial strains has turned to a serious challenge in medicine. Nanomaterials have attracted the researchers' interest due to their significant antibacterial activity. Antibiotics have been a mainstay of human health. They have been

extensively used in clinics to treat respiratory tract infections, urinary tract infections, gastrointestinal infections and infections of nervous system (Singh *et al*., 2014).

Fe_3O_4 nanoparticles have a high specific surface area, so they are able to interact with bacterial surface structures. Furthermore, because of their relatively small size, they can facilitate the particle uptake by bacterial cells (Hufschmid *et al*., 2015). Fe_3O_4 NPs-based biomedical applications have received considerable attention due to their ease of laboratory synthesis, cost effectiveness, physical and chemical stability, as well as biocompatibility and environmental safety (Hui *et al*., 2008). Therefore, Fe_3O_4-NPs may be reasonable candidates for their potential use as antibacterial therapy. The antibacterial study of Fe_3O_4 nanoparticles synthesized from *Lagenaria siceraria* leaves on two clinically isolated strains namely, *Staphylococcus aureus* and *Escherichia coli* show that ,the nanoparticles have the moderate antimicrobial activity when compare to reference drug the result shows higher antibacterial activity against *Eschesheria coli* whereas moderate activity was revealed against *Staphylococcus aureus,* the inhibitory activities in culture media of the Fe_3O_4 NPs (Kumar *et al*.,2012).

Leaf extract of the evergreen shrub Dodonaea viscosa to synthesize Fe_3O_4 nanoparticles and the antimicrobial activity of synthesized nanoparticles was evaluated against human pathogens, namely, *E. coli, K. pneumoniae, P. fluorescens, S. aureus, and B. subtilis*. A very low concentration of synthesized nanoparticles was sufficient to display effective antimicrobial activity as compared to earlier reports (Kiruba *et al*., 2013). The green synthesis of Fe_3O_4 nanoparticles at room temperature using the leaf extract of Tridax procumbens and the synthesized nanoparticles were effective against *Pseudomonas aeruginosa*. The zone of inhibition increased from 1 mm to 2 mm when the concentration of nanoparticles increased fourfold (Senthil and Ramesh, 2012).

Staphylococcus aureus: is a Gram-positive, round-shaped bacterium that is a member of the Firmicutes, and it is a usual member of the microbiota of the body, frequently found in the upper respiratory tract and on the skin. It is often positive for catalase and nitrate reduction and is a facultative anaerobe that can grow without the need for oxygen (Masalha *et al*.,2001*).*

***Escherichia coli* :** Gram-negative bacteria, virulent strain causes food poisoning, urinary tract infection, and neonatal meningitis bacteria. These two different types of pathogenic bacteria have

been chosen for the study because of the above reasons. This work was intended to synthesize Fe_3O_4 nanoparticles synthesize from 'Kosso' *H. abyssinica* flower extract which are cost effective, plant approach and from most common iron salt cheap precursors and investigate the effect of the nanoparticles on bacterial agent against *S. aureus* and *E. coli*. Furthermore, these works also used solgel method to synthesized Fe_3O_4 nanoparticles and compared its effect against the same bacterial strains with nanoparticles synthesized by green method.

2.4.2. Methods for anti bacterial activity test

A variety of laboratory methods can be used to evaluate onscreen the in vitro antimicrobial activity of an extract or a pure compound. The most known and basic methods are the disk-diffusion and broth or agar dilution methods.

Disk diffusion refers to the diffusion of an antimicrobial agent of a specified concentration from disks, into the solid culture medium that has been seeded with the selected inoculum isolated in a pure culture. Disk diffusion is based on the determination of an inhibition zone proportional to the bacterial susceptibility to the antimicrobial present in the disk. The diffusion of the antimicrobial agent into the seeded culture media results in a gradient of the antimicrobial. When the concentration of the antimicrobial becomes so diluted that it can no longer inhibit the growth of the test bacterium, the zone of inhibition is demarcated. The diameter of this zone of inhibition around the antimicrobial disk is related to minimum inhibitory concentration (MIC) for that particular bacterium/antimicrobial combination; the zone of inhibition correlates inversely with the MIC of the test bacterium. Generally, the larger the zone of inhibition, the lower the concentration of antimicrobial required to inhibit the growth of the organisms. Disk-diffusion assay offers many advantages over other methods simplicity, low cost, the ability to test enormous numbers of microorganisms and antimicrobial agents, and the ease to interpret results provided (Jeffrey *et al*., 2008).

Dilution methods are the most appropriate ones for the determination of MIC values, since they offer the possibility to estimate the concentration of the tested antimicrobial agent in the agar (agar dilution) or broth medium (macro dilution or micro-dilution). Either broth or agar dilution method may be used to quantitatively measure the invitro antimicrobial activity against bacteria and fungi. MIC value recorded is defined as the lowest concentration of the assayed

antimicrobial agent that inhibits the visible growth of the microorganism tested, and it is usually expressed in mg/mL or mg/L.There are many approved guidelines for dilution antimicrobial susceptibility testing of fastidious or non-fastidious bacteria (Faller *et al*., 2004).

Broth dilution method: Broth micro- or macro-dilution is one of the most basic anti microbial susceptibility testing methods. Broth di1ution is a technique in which containers ho1ding identical volumes of broth with antimicrobia1 so1ution in incrementally (usua11y geometrica11y) increasing concentrations are inocu1ated with a known number of bacteria. It involves preparing two-fold dilutions of the antimicrobial agent in a liquid growth medium dispensed in tubes containing a minimum volume of macro dilution or with smaller volumes micro dilution (Yamamoto, 2001).

The MIC is the lowest concentration of antimicrobial agent that completely inhibits growth of the organism in tubes or micro dilution wells as detected by the unaided eye. The agar dilution method involves the incorporation of varying desired concentrations of the antimicrobial agent into an agar medium (molten agar medium), habitually using serial two-fold dilutions, followed by the inoculation of a defined microbial inoculum onto the agar plate surface. The MIC endpoint is recorded as the lowest concentration of antimicrobial agent that completely inhibits growth under suitable incubation conditions. This technique is suitable for both antibacterial and antifungal susceptibility testing. If multiple isolates are being tested against a single compound, or if the compound (or extract) tested masks the detection of microbial growth in the liquid medium with its coloring, agar dilution method is often preferred to broth dilution for the MIC determination(Yamamoto, 2001). In this studies disk diffusion method was used for anti bacterial activity.

2.4.3. Anti bacterial mechanism of Fe_3O_4 nanoparticles

The antimicrobial mechanisms of NPs involve three model oxidative stress induction, metal ion release, or non-oxidative mechanism. The advantage of the NPs is that these three mechanisms can occur simultaneously (Wang *et al*., 2017). Subsequently, NPs damage the basic components of the bacterial cell such as DNA, lysosomes, ribosomes, enzyme inhibition, proteins deactivation, changes in cell membrane permeability, and changes in genes expression that

ultimately leads to cell death (Xu *et al*., 2016). So, there is dire need to focus on biocompatible NP-based material with antibacterial activity.

Due to difference in the cell walls of Gram +ve and Gram −ve the action of NPs dependent on bacterial strains (Tran *et al*., 2010). The mechanism involves electrostatic interaction between bacterial cell wall and NPs which deteriorate cell wall of bacteria and induces toxic oxidative stress by producing reactive oxygen species (Ahmad *et al*., 2014). The bactericidal effects of Fe_3O_4 NPs provide high bioactivity even if small dose is used. Contrarily, the action of antibiotics attacks three bacterial sites that are; Cell wall, translational machinery and DNA replication, due to this reason bacterial resistance develop against each one of these modes of actions (Woolhouse *et al*., 2015).

The modes of action of NPs develop a direct contact with the bacterial cell wall that damages the bacterial cell without penetration to the cell. Therefore, NPs are less prone to bacterial resistance than antibiotics (Wang *et al*., 2017). Biocompatibility and magnetic properties of Fe_3O_4 NPs make it promising material against every type of pathogens (Li *et al*., 2012). In addition, positive surface charge of the metal NPs promote their binding to the negatively charge surface of bacteria which enhance antimicrobial activity of Fe_3O_4 NPs (Seil and Webster, 2012). Figure 3 shows schematic representation of mechanism of interaction of IONPs with bacterial strains.

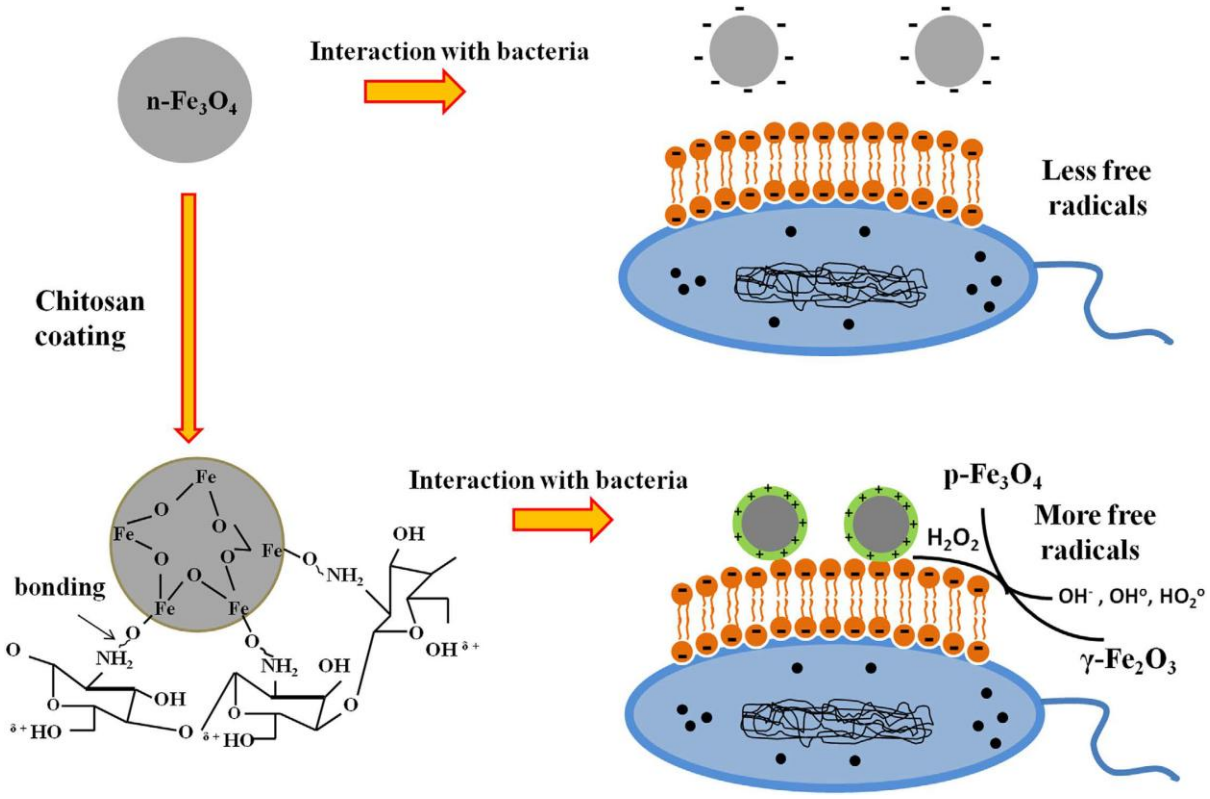

Figure 3. Proposed schematic model elucidating the detail mechanism of iron oxide nanoparticles against bacterial cells (Manoranjan *et al.*, 2015*)*

3. MATERIALS AND METHODS

Experimental Sites:- Green synthesis of Fe_3O_4 nanoparticles using flower extract *of H. abyssinica*and chemically synthesized Fe_3O_4 nanoparticles using solgel method, characterization of the both synthesized Fe_3O_4 nanoparticles using XRD and Antibacterial Activity was done at Adama Science and Technology University. Characterization of the both synthesized nanomaterials using SEM-EDS and UV-Vis spectroscopy was done at india and characterization of the synthesized nanoparicles using FTIR spectroscopy was done at Addis Ababa University, department of Chemistry.

3.1. Apparatus and Equipments

The apparatus and equipments used during this research work were:- FTIR (Perkin Elmer 65), XRD(XRD-7000,shimadzuco South Korea), UV-Vis spectrophotometer(JASCO V-78 UV-Vis spectrophotometer equipped with a diffuse reflectance attachment for powder samples) and SEM-EDX(FESEM, JEOL-JSM 8040,81F made in Japan).

3.2. Chemicals and Reagents

In this research work different chemicals and reagents were used, such as distilled water, ferric chloride hexahydrate (Sigma Aldrich), ferrous sulphate heptahydrate (Sigma Aldrich), ethanol(99.9%; Blulux Ltd, Ranchem Industry and Trading), sodium hydroxide (Sigma Aldrich), ferric nitrite (Sigma Aldrich) and ethylene glycol (Sigma Aldrich).

3.3. Synthesis of Fe_3O_4 NPs by Chemical Method

Ferric nitrate ($Fe(NO_3)_3.9H_2O$) and ethylene glycol ($C_2H_6O_2$) were used for the preparation of magnetic nanoparticles in this present study. Exactly 0.1 M of ferric nitrite was dissolved in 25 ml ethylene glycol and placed in magnetic stirrer for 2 hours at 75°C to obtaining brown gel. Then the gel was kept in oven at 250°C temperatures for drying. After drying, the xerogel was annealed at 250°C (Aftabtalab and Sadabadi, 2015).

The reaction principles as follows

$6\ Fe(NO_3)_3.9H_2O + 46\ C_2H_6O_2 \rightarrow 2\ Fe_3O_4 + 92\ CO_2 + 192\ H_2O + 9\ N_2$ (Sara *et al*., 2013) .

3.4. Synthesis of Fe_3O_4 NPs by Green Method

3.4.1. Collection and Preparation of Plant Material

Fresh plant flowers of *Hagenia abyssinica* were collected from Arsi zone Oromia region in Autumn season by Meko Dube. The collected plant flowers were then washed for removing dust and any impurities by using distilled water and dried at room temperature under shade. The dried flowers were chopped and then ground into powder. Then, the ground powder were sieved using 250 μm dimeter sized seive. The plant powder (5g) were extracted by boiling 100 ml of water in 250 mL glass flasks at 60 ^oC for 40 minutes. Then the resulted dark brown colored extract was cooled to room temperature and filtered before to remove any heavy biomaterials. Finally, the extract was kept at 25 ^oC in order to be used for the synthesis of the target magnetic nanoparticles (Nurbas *et al*. 2017).

Figure 4 (a-d) shows the schematic preparation processes of *H.abyssinica* flower extract respectively.

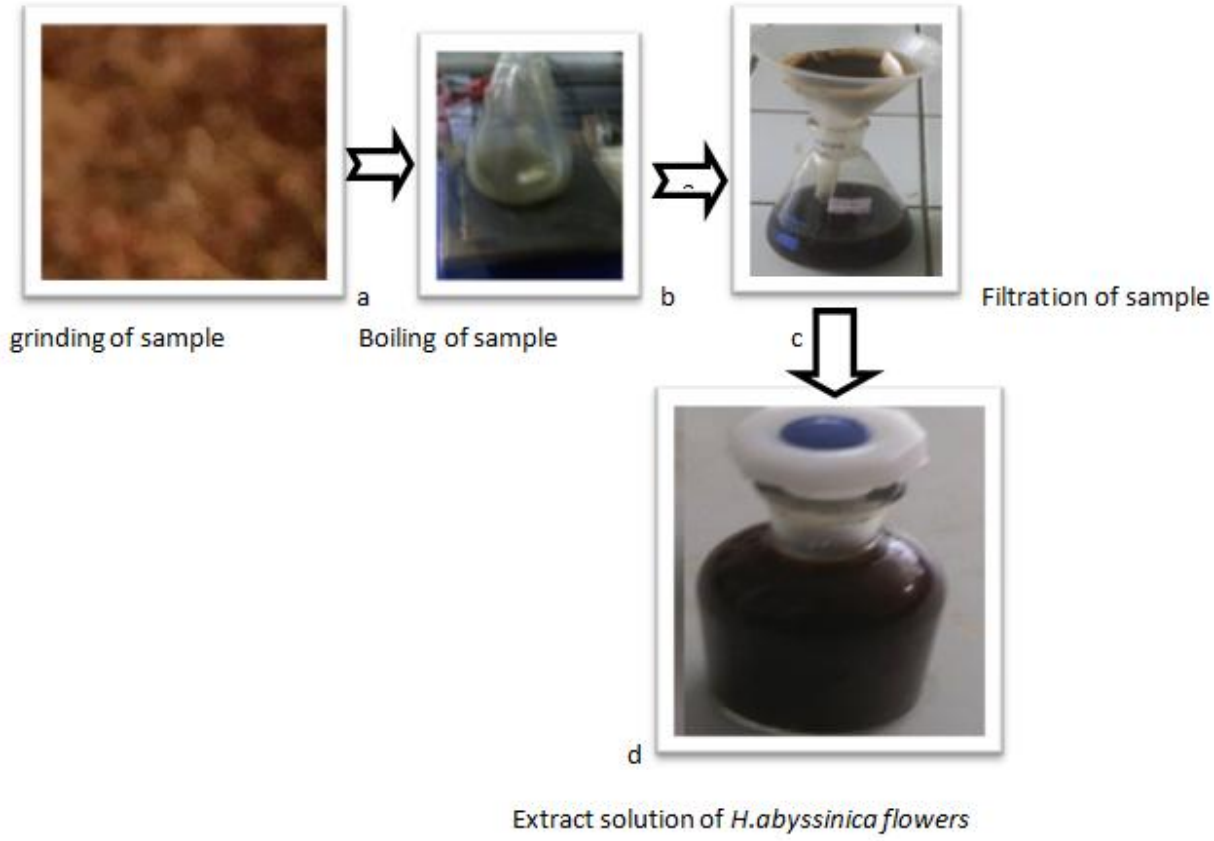

Figure 4. The preparation process of *H.abyssinica* flower extract.

3.4.2. Synthesis of Fe_3O_4 Nanoparticles

The synthesis of the magnetic nanoparticles was carried out by an improved biosynthesis method(by using plant extract within different ratio). This procedure was used by modifying few things (concentration and substitution of $FeCl_2.4H_2O$ by $FeSO_4.7H_2O$). To do so, $FeSO_4.7H_2O$ and $FeCl_3.6H_2O$ at 1:2 molar ratios were dissolved in water by stirring at the speed of 700 rpm for 2 h. Then, flower extract was added to the metal ions solutions. After the addition, the color of the solution started to change in a short time from yellow to black. The color change represents the formation of nanoparticles which can be seen in Figure 5. Then, 2.0 M of NaOH solution was added to the metal ion solution until the pH value was attained to 11. The specimens were filtered to remove the solid product and washed by ethanol. Finally, the specimens was dried in an oven at 50^{o}C and calcinated at 400 ^{o}C prepared for the characterization (Nurbas *et al*. 2017).

In a typical experiment, the extract was added to ferric chloride and ferrous sulphate precursor solution in three different ratios by volume.

For **1:1 ratio**: 50 mL of 0.1 M Ferrous sulphate heptahydrate, 0.2 M Ferric chloride hexahydrate and 50mL of *H.abyssinica* flower extract.

For **1:2 ratio**: 0.1 M Ferrous sulphate heptahydrate, 0.2 M Ferric chloride hexahydrate 33.3 mL and 67.7 mL of *H.abyssinica* flower extract.

For **2:1 ratio**: 0.1 M Ferrous sulphate heptahydrate, 0.2 M Ferric chloride hexahydrate 66.7 mL and 33.3 mL of *H.abyssinica* flower extract.

The proposed reaction scheme was:

$Fe^{2+} + 2Fe^{3+} + \text{extract} + 8OH^- \leftrightarrow Fe(OH)_2 + Fe(OH)_3 \rightarrow Fe_3O_4 + 4H_2O$

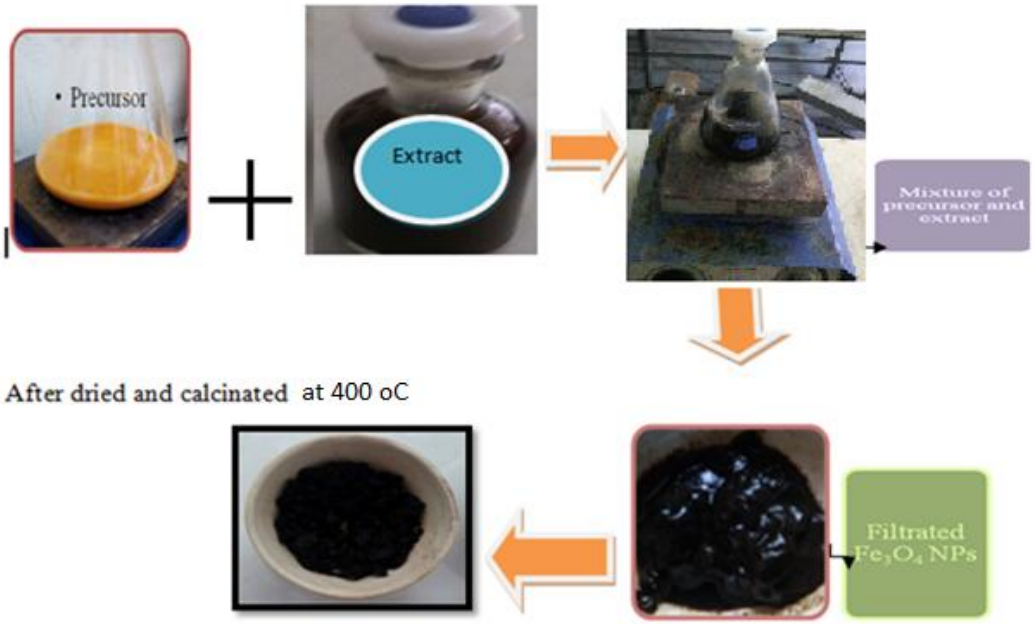

Figure 5: Schematic representation of synthesis process for Fe_3O_4 nanoparticles.

3.5. Characterization of Fe_3O_4 Nanoparticles Using X-ray diffractometer (XRD)

To analyze structure of the synthesized Fe_3O_4 Nps XRD was employed. The XRD pattern of Fe_3O_4 Nps was recorded on X-ray diffractometer at the range of 2θ from 10 to 80 with a scan

rate of 20/ min using Cu Kα (λ = 1.5406 A^0) radiation with an accelerating voltage of 40 KV. Different phases present in the samples was evaluated (Saqib *et al.,* 2018). The average particle size was calculated with Debye Scherrer's formula.

$$D = \frac{0.94\lambda}{\beta\cos\theta} \text{ ---------- (1)}$$

Where, D the Crystallite size, λ = 1.54 A^0 is the X – ray source wavelength, β is the Full Width at Half Maximum (FWHM) of a peak, and θ is the peak position (Arokiyaraj *et al.,* 2013).

3.6. Characterization of Fe_3O_4 Nanoparticles Using Scanning Electron Microscope and Energy-Dispersive X-ray Spectroscopy (SEM-EDS)

The scanning electron microscopy was carried out to study the surface morphology of Fe_3O_4 NPs. The nanoparticles was taken and mounted with double adhesive tape on stubs, sputter coated with gold palladium. To analyze morphological features of Fe_3O_4 NPs field emission scanning electron microscope was used at an accelerating voltage of 10 KV upon gold coating for 4 min. The chemical composition of the biosynthesized Fe_3O_4 NPs nanoparticles was estimated by energy-dispersive X-ray spectroscopy. Energy dispersive X-ray analysis attached with SEM determined presence of different elements in the NPs sample. The specimen was determined through energy-dispersive X-ray spectroscopy software that applies ZAF correction and carries out subsequent integration of the peaks to get the final quantification of the elements present in the sample (Saqib *et al.,* 2018).

3.7. Characterization of Fe_3O_4 Nanoparticles Using Fourier Transform Infrared (FTIR)

The prepared Fe_3O_4 nanoparticles was subjected to FT-IR spectroscopy measurements. It was recorded by using spectrometer in the range 400 - 4000 cm^{-1} at a resolution of 4 cm^{-1} based on KBr pellet technique. It was used to identify the possible biomolecules/functional groups adhered to the surface of the nanoparticles and which might have acted as capping agents of the nanoparticles (Kumar and Ananthu, 2018).

3.8. Characterization of Fe_3O_4 Nanoparticles Using UV-Vis Spectroscopy

The surface plasmon resonances (SPR) of synthesized iron oxide nanoparticles have been studied by UV-Vis Spectrophotometer. The absorption of visible radiations due to the excitation of SPR, imparts various colours to nanoparticles. As the nanoparticles size changes, colour of the solution also changes. So UV-Vis absorption spectrum is quite sensitive to the formation of nanoparticles. The UV-Vis absorption spectra of the Fe_3O_4 nanoparticles from *Hagenia abyssinica* flower extract and that of chemically synthesized was confirmed by using wave length scan between 200 nm and 800 nm (Bhosale *et al*., 2014). From the UV-Vis graphs, energy band gap was obtained using the formula: $Eg = 1240/\lambda_{max}\ eV = \frac{hc}{\lambda}$ ---------- (2)

Where Eg is energy band gap, h is planks constant, c is speed of light and λ is the maximum wavelength of the synthesized Fe_3O_4 nanoparticles.

3.9. Method for Antibacterial Activity

Materials used for antimicrobial activity of Fe_3O_4 NPs were 0.2 g nutrient broth, Erlenmeyer flask, Cotton, autoclave, Petri plates, Fe_3O_4 NPs, 2 g agar, *Staphylococcus aureus* and *Escherichia coli*. Disc diffusion method were used for antimicrobial activity of iron oxide(Fe_3O_4) nanoparticles.

3.9.1. Preparation of Inoculum

0.2 g nutrient broth was dissolved in 25 mL distilled water prepared in two Erlenmeyer flasks. Cotton plugs the flask and sterilized it in autoclave at 121 ^oC for 15 min. In one conical flask clinically isolated strain of *Staphylococcus aureus* was inoculated. In the other conical flask clinically isolated strain of *Escherichia coli* was added. Inoculums of all the strains were developed in this growth media. A loop full of bacterial strain was added in it and it was left over night at 37^oC in shaking incubator. This was diluted before inoculating the plates (Gupta and Gupta, 2005).

3.9.2. Disc diffusion Method for Antimicrobial Activity

2 g agar and 0.8 g nutrient broth were mixed to make 100 mL solution in an Erlenmeyer flask. Cotton plugs the flask and sterilized it. Poured about 15 to 20 ml of agar in Petri plate, solidified it and then inoculate it with the bacterial strain. Wells having diameter of 0.4 cm will be developed in which 10 µL of sample suspension was added. Suspensions of all samples were prepared by dissolving 25µg, 50 µg and 75µg of product in1 mL DMSO. These plates was kept for 24 hours at 37 ^{o}C and zones of inhibition was observed (Gupta and Gupta, 2005).

4. RESULTS AND DISCUSSION

4.1. X-ray Diffraction (XRD) Analysis

Figure 6(a, b and c) shows the XRD spectrum of Fe_3O_4 NPs green synthesized from ferric chloride hexa hydrate and ferrous sulphate hepta hydrate precursor and flower extract of *H. abyssinica* using 1:1, 1:2 and 2:1 ratios respectively. As shown in Figure 6 the formation of Fe_3O_4 Nanoparticles was analyzed by x-ray diffraction. The diffraction peaks of the synthesized Fe_3O_4 Nanoparticles (Figure 6a) where detected at $2\Theta = 30.37^o$, 35.73^o, 43.33^o, 57.22^o, and 62.95^o , which are assigned to the crystal planes of (220), (311), (400), (511) and (440), respectively.

Again as shown in Figure 6(b) Fe_3O_4 (1:2) nanoparticles, the peak were observed at $2\Theta = 30.24^o$, 35.57^o, 43.24^o, 58.02^o and 62.68^o which corresponding miller index values of (220), (311), (400), (422) and (440), respectively. Similarly, for Fe_3O_4 (2:1) NPs (Figure 6(c)) the peaks where observed at $2\Theta = 30.20^o$, 35.59^o, 43.18^o, $57.57.13^o$ and 62.72^o, which were assigned to the crystal planes of (220), (311), (400), (511) and (440) respectively. Those results reveals that the green synthesis NPs have possessed good crystallinity in nature and also diffraction peaks related to impurities were not observed in the XRD pattern, confirming the purity of the green synthesized nanomaterials. The average crystalline size of the green synthesized Fe_3O_4 NPs within 1:1, 2:1 and 1:2 ratios were found to be 8, 8.3 and 9.2 nm, respectively.

Estimation of the crystallite size of synthesized Fe_3O_4 NPs were calculated by using the Debye-Scherrer equation, $D = \frac{K\lambda}{\beta Cos\Theta}$ (Yuvakkumar and Hong, 2014). The green synthesized Fe_3O_4 nanoparticles were approximately matched with that of synthesized by using *Couroupita guianensis Aubl*. extract and the average crystalline size calculate was 7.2 nm, the reflection peak position and relative intensities were approximately matched within the standard magnetite of Fe_3O_4 at $2\Theta = 35.54^o$, this was confirm the inverse cubic spinel structure (Sathishkumar *et al.*,2018).

Fe_3O_4 nanoparticles green synthesized using a 1:1 ratio showed that the average crystalline size has relatively smaller particle size (8 nm) as compared to the average crystalline size of Fe_3O_4

synthesized using 2:1 (8.3 nm) ratio. This difference may be due to the fact that the greater amount of *H. abyssinica* flower extract used during the synthesis process results in a more capping agents that intern effectively stabilize the green synthesized Fe_3O_4 (1:1) nanoparticles. Fe_3O_4 nanoparticles was also synthesized using a 1:2 ratio. The average crystalline size is greater than that synthesized using 1:1 ratio. In green synthesized of Fe_3O_4 nanoparticles good result was obtained when the ratio of precusor used and plant extract used was equal. When the plant extract was greater than precusor used the crystalline nature of of the particle lost and when the precusor used was greater than that of plant extract, there was high yield of sample and its have good crystalline nature

As show in Figure 6 (d) the formation of iron oxide (Fe_3O_4) nanoparticles by chemical method was analyzed. The diffraction peaks were in a good agreement with the one which was reported with JCPDS Card No. 79 - 0417. The peaks were observed at $2\Theta = 30.27^o$, 35.59^o, 43.30^o, 57.34^o and 62.82^o with miller indices values of (220), (311), (440), (511) and (440), respectively. Similar result was also reported that Fe_3O_4 nanoparticles were synthesized using ferric nitrate precursory and ethylene glycol (Jing *et al*., 2007). Also the reflection peak position and relative intensities were well matched with the standard magnetite of Fe_3O_4 at $2\Theta = 35.481^o$confirmed that the inverse cubic spinel structure and the average crystallite size was calculated to be 10.6 nm.

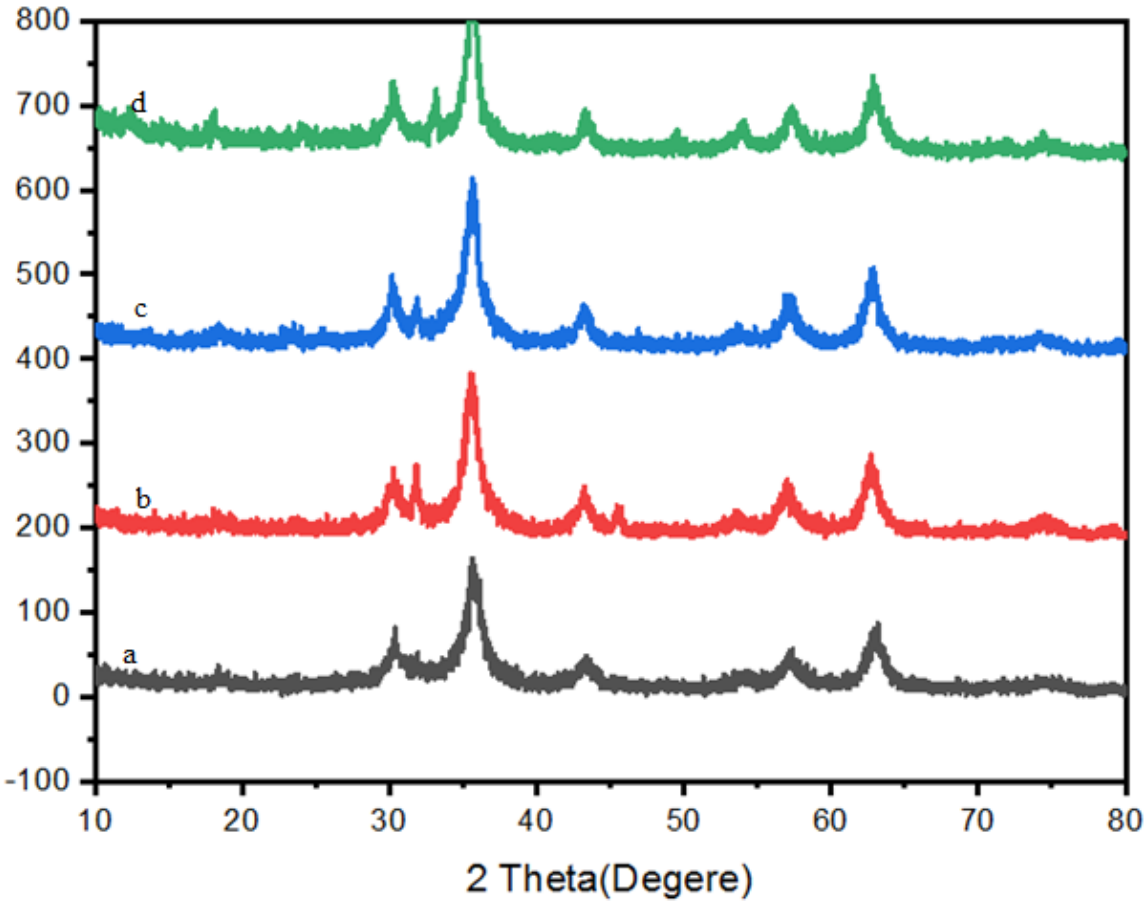

Figure 6: XRD Spectrum of green synthesized Fe_3O_4 NPs using: (a) 1:1, (b) 1:2, (c) 2:1 and (d) chemically synthesized Fe_3O_4 NPs.

From the XRD spectrum of Fe_3O_4 nanoparticles NPs synthesized using plant extract and chemically synthesized Fe_3O_4 nanoparticles, the average crystalline size of the former was smaller than the latter .This due to the presence of reducing and capping agents from the plant extract that can stabilize and has potential to minimize agglomeration of the nanoparticles. Table 1 and 2 show summary of parameters extracted from the XRD spectra of the synthesized nanoparticles using both green and chemical methods.

Table 1: Different angles, interplanar spaces (d-hkl), FWHM values, lattice plance, lattice parameter and sizes of Fe_3O_4 nanoparticles for S11 and S12.

Fe_3O_4 NPs (S11)						Fe_3O_4 NPs (S12)					
2θ	d-hkl	FWHM	Hkl	"a" (Å)	size (nm)	2θ	d-hkl	FWHM	Hkl	"a" (Å)	size (nm)
30.3729	2.94051	0.78000	220	8.32	10.2	30.2496	2.95222	0.89330	220	8.35	8.9
35.7322	2.51081	1.11000	311	8.47	7.2	35.5724	2.52172	1.03000	311	8.36	7.7
43.3317	2.08644	1.04000	400	8.35	7.7	43.2418	2.09057	0.78000	400	8.36	10.2
57.2253	1.60853	1.12000	511	8.36	7.1	58.0250	1.58825	0.48000	511	8.30	16.6
62.9584	1.47514	1.15000	440	8.34	6.9	62.6834	1.48095	1.08000	440	8.38	7.4
Average lattice parameter **8.37** Average crystallite size **7.82**						Average lattice parameter **8.35** Average crystallite size **10.16**					

Table 2: Different angles, interplanar spaces (d-hkl), FWHM values, lattice plane, lattice parameter and sizes of Fe_3O_4 nanoparticles for S21 and chemically synthesized samples.

Fe_3O_4 NPs (S21)						Fe_3O_4 NPs synthesized by chemical method					
2θ	d-hkl	FWHM	Hkl	"a" (Å)	size (nm)	2θ	d-hkl	FWHM	Hkl	"a" (Å)	size (nm)
30.2081	2.95618	0.79000	220	8.36	10	30.2780	2.94951	0.75000	220	8.34	10.6
35.5907	2.520947	1.02670	311	8.36	7.76	35.5989	2.51990	0.82330	311	8.36	9.7
43.1818	2.09334	0.94000	400	8.37	8.5	43.3017	2.08782	0.74000	400	8.35	10.7
57.1303	1.61097	1.03000	511	8.37	7.7	57.3478	1.60538	0.96500	511	8.34	8.2
62.7234	1.48010	1.08000	440	8.37	7.4	62.8234	1.47798	1.08000	440	8.4	7.4
Average lattice parameter **8.37** Average crystallite size **8.3**						Average lattice parameter **8.36** Average crystallite size **9.3**					

The lattice parameter "a_o" of Fe_3O_4 nanoparticles from XRD result is determined by (Chaki *et al*., 2015):

$$d_{hkl} = \frac{a}{\sqrt{h^2 + k^2 + l^2}} \quad ----------(3)$$

4.2. SEM-EDS Analysis

Morphology of Fe_3O_4 nanoparticles were studied using SEM images. The surface morphology of synthesized Fe_3O_4 nanoparticles samples was viewed through the high resolution scanning electron microscope. Figure 7(a,b and c) shows the SEM images of green synthesized Fe_3O_4 nanoparticles(1:2 and 1:1) ratios and chemically synthesized Fe_3O_4 nanoparticles. The green particles were found to be flower in shape with distinct edges and that of chemically synthesized was SEM image of rod shape. The morphology of the green synthesized of Fe_3O_4 nanoparticals was found to be homogeneous in some specific region. The morphology of Fe_3O_4 nanoparticals synthesized from ferrous heptahydrate, ferrric hexahydrate and from extract of *H. Abyssinica* and Fe_3O_4 nanoparticals synthesized from ferric nitrate and ethylene glycol have cubic spinel structure.

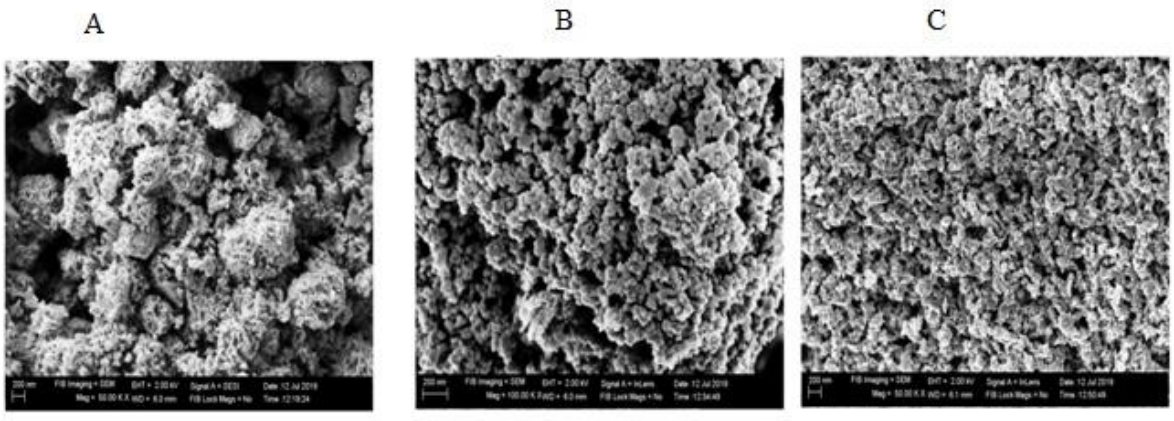

Figure 7: SEM images of Fe_3O_4 nanoparticles for (a) green uncalcinated, (b) green calcinated and (c) chemically synthesized.

The result of the SEM image confirms the particle size of uncalcinate Fe_3O_4 (figure 8a) nanoparticles was larger than that of calcinate Fe_3O_4 nanoparticles (8b) and also the result proves that the synthesized nano particles are crystalline in nature and indeed metallic Fe_3O_4 nanoparticles which agrees with that of the XRD results obtained, i.e the particle that have small size in XRD have also small grain in SEM images and that of big particle size have big SEM image. Energy dispersive x-ray spectroscopy (EDS) shows elements that are present in magnetite nanoparticles (Figure 8). It was necessary to verify the presence of desired elements in the green

synthesized and chemically synthesized nano sample by using energy dispersive x-ray spectroscopy (EDS).

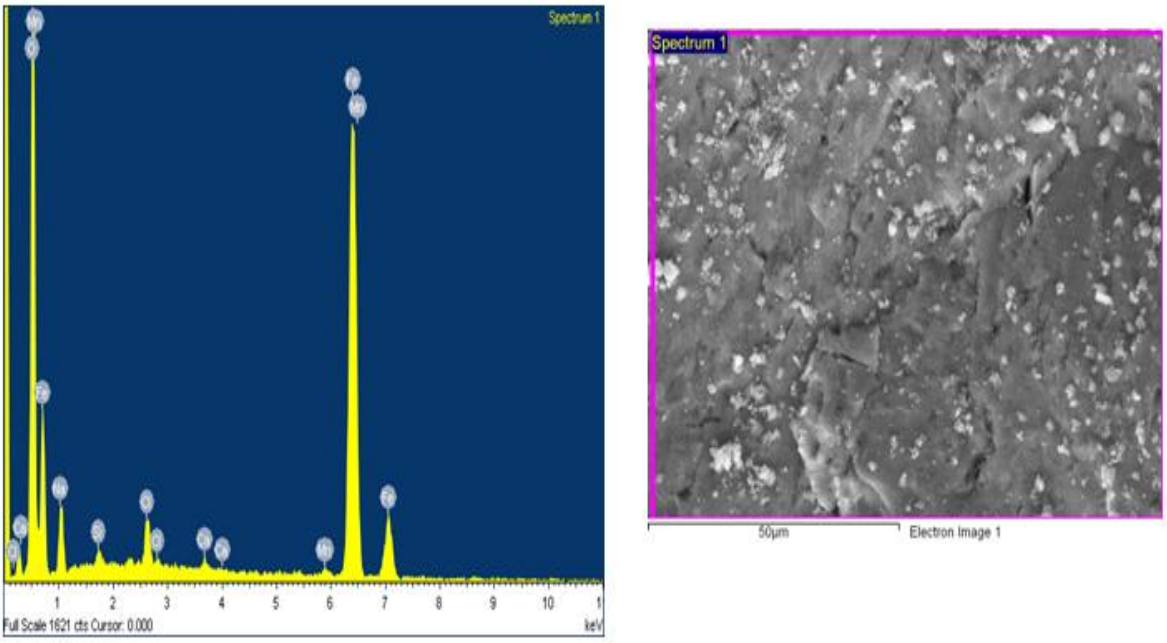

Figure 8: EDS spectra of uncalcinated (a) and SEM images of selected EDS spectra for uncalcinated samples.

.

Table 3: Shows quantitative analysis of green uncalcinated Fe_3O_4 nanoparticles

Element	Weight %	Atomic %
O K	36.20	63.04
Na K	5.99	7.26
Si K	0.51	0.50
Cl K	1.87	1.47
Ca K	0.36	0.25
Mn K	0.65	0.33
Fe K	54.42	27.15
Total	100	

The presence of other elements/foreign materials other than iron and oxygen on the green synthesized nano sample occurred from the standard of SEM instrument... The elemental composition of green synthesized Fe_3O_4 nanoparticles calcinated (b) was also determined by energy dispersive x-ray spectroscopy (EDS) using scanning electron microscopy. It shows the presence of Fe and O and also it shows other material that found in Fe_3O_4 nanoparticles composition. The weight % for iron and oxygen were 52.75% and 34.37% respectively giving a total of 87.12% and also the atomic % were 25.61% and 58.26% respectively giving a total of 83.87%. The total weight % and atomic % for other components were 12.88% and 16.13% respectively.

The elemental composition of chemically synthesized Fe_3O_4 nanoparticles determined by energy dispersive x-ray spectroscopy using scanning electron microscopy. From Figure 9 blow, the x-ray patterns of chemically synthesized Fe_3O_4 nanoparticles in which Fe and O were found in the

respective EDS spectrum and in addition to this there was a C present in the spectrum. Similar result also reported by (Sara *et al*., 2013).

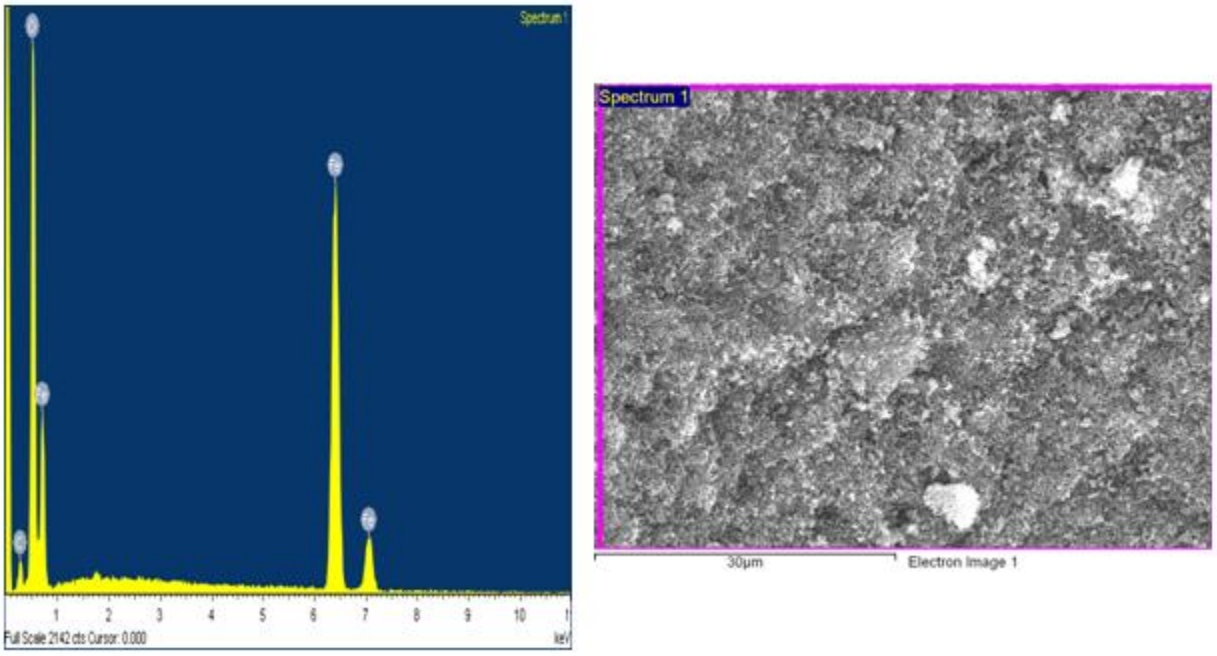

Figure 9: EDS spectra and SEM images of selected EDS spectra for sample(c) for chemically synthesized Fe3O4 nanoparticles.

Table 4: Shows quantitative analysis of chemically synthesized Fe_3O_4 nanoparticles

Element	Weight%	Atomic%
C K	6.87	14.12
O K	40.61	62.66
Fe K	52.51	23.21
Totals	100.00	

4.3. Fourier Transform Infrared (FTIR) Analysis

Figure 10 shows the FT-IR spectra of Fe_3O_4 nanoparticles synthesisized using plant extract for uncalcinated (a) and calinated (b) and Fe_3O_4 nanoparticles chemically synthesized (c), respectively. The FTIR spectrum of green synthesized uncalcinated iron oxide magnetite nanoparticles showed peaks at 3437.3, 2926.1, 2841, 1617.82, 1414.17, 1334, 871, 788 and 598 cm^{-1}. From those indicated peaks, the broad absorpiton peak of iron oxide (Fe_3O_4) nanoparticles observed at 3437.3 cm^{-1} represents the presence of alcohols, phenols with O-H stretchs. The absorption peak indicated at 1617.82 cm^{-1} represents the C=O stretching of primary amide or C=C groups of aromatic rings. The peaks at 1334 cm^{-1} and 1414.17 cm^{-1} are attributed to the vibration of the double covalent bond in –CH = CH-. The peak at2841, 871 and 788 cm-1 represents C-H bond stretch. The peak at 2926.1 also represent $–CH_2$ asymmetric stretch and the peaks at 598 cm^{-1} represents peak of Fe-O bending mode of vibration which confirms formation of metal oxygen bonding.

Figure 10 (b) shows the FT-IR spectrum of calcinated synthesized Fe_3O_4 NPs showed peaks at 3455, 2920, 2836, 1395.5, 1113.43, 885 and 573.8 cm^{-1}. The broad absorption peaks of magnetite nanoparticles observed at 3455cm^{-1} indicates the presence of alcohols, phenols with O-H stretches and also the peaks at 1395.5 cm^{-1} attributed to O-H bend. The peak at 2920 cm^{-1} represents $–CH_2$ asymmetric stretch of alkene. The peak at 1113.43 cm^{-1} was attributed to the vibration of the covalent bond in C-O stretch. The peak at 885 cm^{-1} represents alkenes CH_2=CH- stretch. The peak at 2836 cm^{-1} represents C-H bond stretch and the peaks at 573.8 cm^{-1} represents peak of Fe-O bending mode of vibration which confirms formation of metal oxygen bonding. The peak Fe-O bond for both calcinated and uncalcinated Fe_3O_4 nanoparticles formed from region 400 to 600 cm^{-1}(Yuvakkumar and Hong, 2014).

As seen from the Figure (10 a and b) for uncalcinated Fe_3O_4 nanoparticles and calcinated Fe_3O_4 nanoparticles, the peak indicates that there was many organic solvent in uncalcinated Fe_3O_4 nanoparticles as compared to that of calcinated Fe_3O_4 nanoparticles. After calcination of Fe_3O_4 nanoparticles, the band peak at 1617.82, the band peak at 1334 and the band peak at 871 removed from the spectrum of Fe_3O_4 nanoparticles. The spectrum of calcinated Fe_3O_4

nanoparticles indicates that the organic solvent was eliminated after the calcination of the sample.

Figure 10 (c) shows the FT-IR spectrum of chemically synthesized Fe_3O_4 NPs showed peaks at the 3388.8, 2340, 1622.38, 1401.29 and 560 cm^{-1} respectively. From those indicated peaks, the broad absorption peak of iron oxide nanoparticles observed at 3388.8 cm^{-1} represents the presence of alcohols, phenols with O-H stretches. The peak at 2340 cm^{-1} indicates alkene group with C=C stretching. The peaks at 1401.29 cm^{-1} attributed to the vibration of the bond in O-H stretching vibrations of H_2O molecules, indicating higher amount of surface hydroxyl groups, while those at 1622.38 cm^{-1} are associated with their bending mode. Generally, the H_2O and CO_2 molecules are easily chemisorbed onto Fe_3O_4 surface when exposed to the atmosphere and from those indicated peaks, the broad absorption peak of iron oxide nanoparticles observed at 560 cm^{-1}. However, Fe_3O_4 has inverse type spinel structure and it has been observed that spinel type structure exhibit mainly two absorption bands at ~ 600 and ~450 cm^{-1} corresponding to the metal –oxygen (Fe-O) band in tetrahedral octahedral sites. This result is constituent with other studies reported by (Srivastava *et al*., 2012). This can be attributed to the high degree of crystalline nature of the Fe_3O_4 nanoparticles (Rahman *et al*., 2012).

Generally, from FTIR specta of Fe_3O_4 nanoparticles synthesized using both chemical and green method , in green method there was many peaks as seen from Figure 8(a and b) as compared to that of chemically synthesized Fe_3O_4 nanoparticles Figure 11 (c) .This indicates there were different organic solvent that found in the flower extract of *H. Abyssinica* that used for the synthesis of green Fe_3O_4 nanoparticles.The FTIR spectra of calcinated Fe_3O_4 nanoparticles was almost similar to that of chemically synthesized Fe_3O_4 nanoparticles. There difference was only at peak of 2340 cm^{-1}. It found on the spectra of chemically synthesized Fe_3O_4 nanoparticles but its not presented in green calcinated Fe_3O_4 nanoparticles.

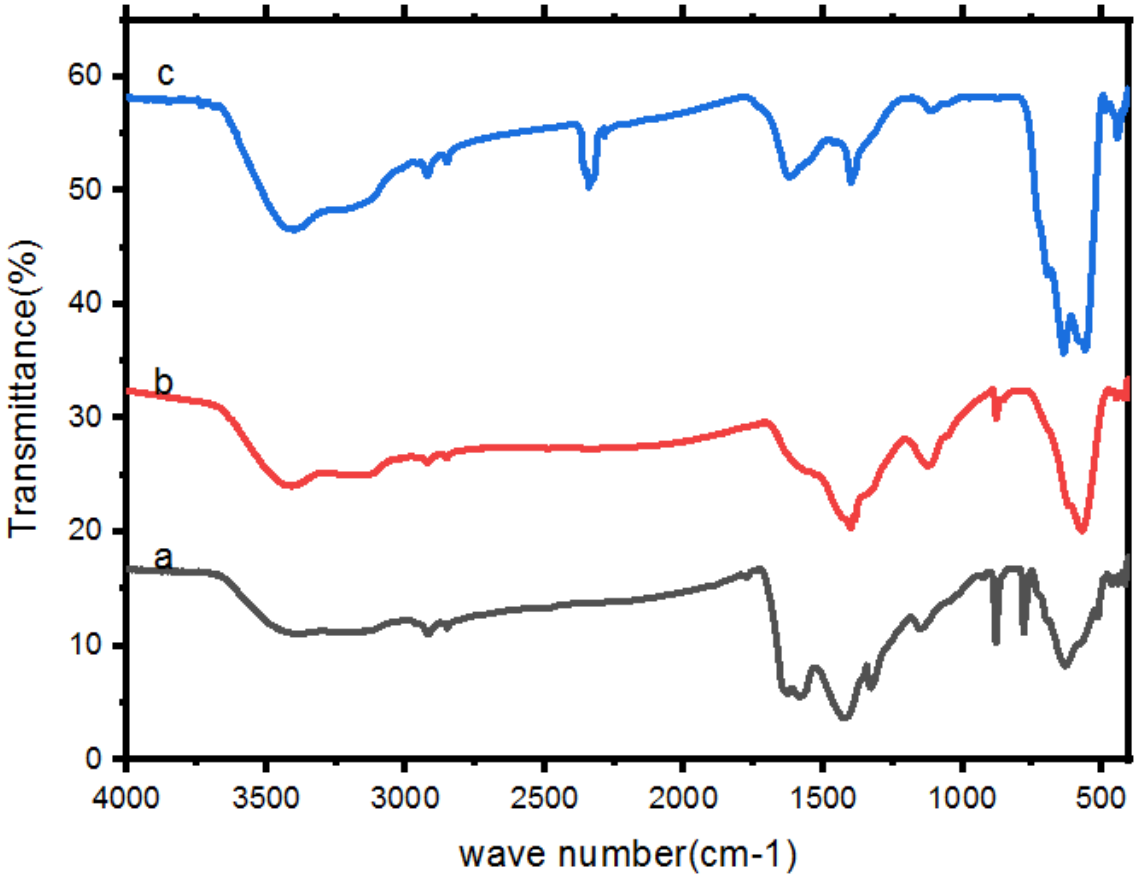

Figure 10. FTIR spectrum of Fe_3O_4 nanoparticles synthesized by green method and chemical method.

Generally, it can be seen that the presence of different amine group , carboxylic acids and the alcohol found in the flower of *H. abyssinica* led to the formation of Fe_3O_4 nanoparticles by acting as reducing and capping agent. How ever these group was absent in chemically synthesized Fe_3O_4 nanoparticles.

4.4. Ultraviolet-Visible Spectroscopy (UV-Vis) Analysis

The reflectance spectra of Fe_3O_4 nanoparticles green synthesized and chemically synthesized are indicated in Figure 11 (A) reveals the reduction process and formation of nanoparticles. Iron oxide (Fe_3O_4) nanoparticles formation was confirmed by the color change immediately occurred after the addition of the plant extract to precursor solution. The mixture color immediately

converted from transparent yellow to black in a few seconds demonstrating the synthesis of iron oxide nanoparticles (Figure 11A). This was confirmed by the appearance of reflectance bands around 324.4 nm for green method (Figure 9a) and around 328.5 nm for that of chemically synthesized (Figure 11b). Both the nanoparticles (green method and chemical method are subjected to uv-vis characterization. In this case the reflectance of green synthesized Fe_3O_4 nanoparticles were few smaller than that of chemically synthesized Fe_3O_4 nanoparticles; this was occurred due to the size of the Fe_3O_4 nanoparticles. The band gap energy of Fe_3O_4 nanoparticle green synthesized and chemically synthesized were determined from the kubelk munk function plot, by using direct band gap method. The graphy was plotted by using $(F(r)\ hv)^2$ vs hv

Where, hv – Energy term

V- Frequency and h- is planks constant

F(r) – is the kubelka munka function

Figure 11(A, B and C) shows the reflectance of Fe_3O_4 nanoparticles and direct band gap respectively.

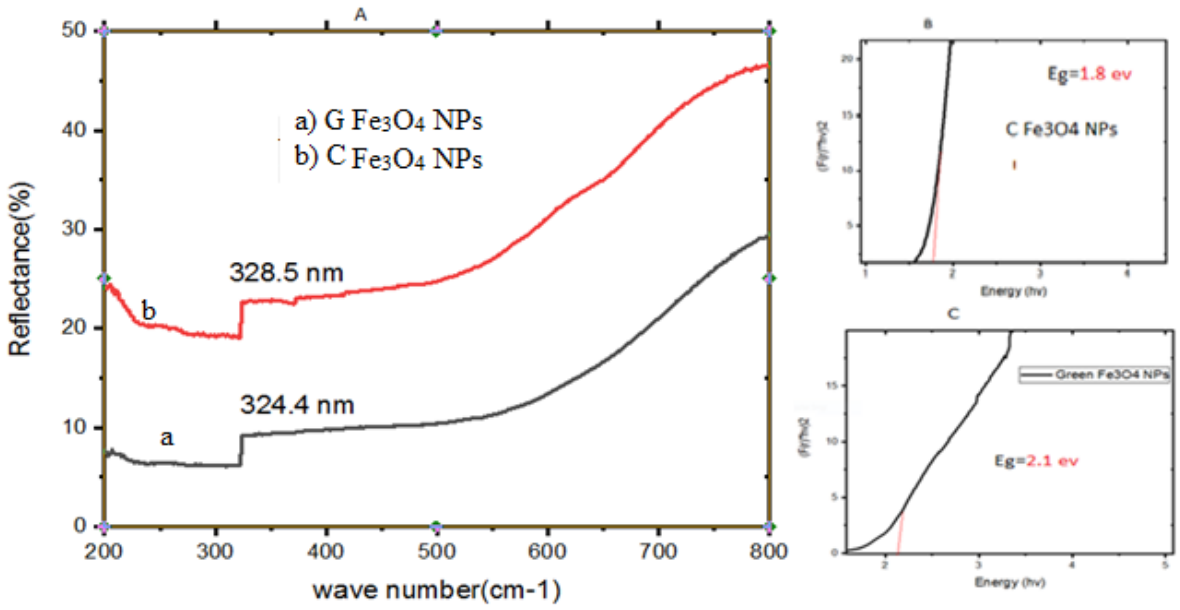

Figure 11: UV-Vis reflectanceof Fe_3O_4 nanoparticles(A) and direct band gap (B and C).

The band gap energy was determined based on the numerical derivative of the optical absorption coefficient. The fundamental reflectance method refers to valence band to conduction band was obtained by using the energy relation formula which is Eg = $\frac{hc}{\lambda}$. There for band gap for green synthesized Fe_3O_4 nanoparticles was 2.1 ev and that of chemically synthesized 1.8 ev. As the nanoparticles size changes, colour of the solution also changes (Bhosale *et al*., 2014). So UV-Vis absorption spectrum is quite sensitive to the formation of nanoparticles. The band gap result obtained in this study was related to that of reported by (Ghandoor *et al*., 2012).

4.5. Antibacterial Activity

Fe_3O_4-NPs exhibit considerable antibacterial effects because of their specific features including their size and larger surface area which facilitates their interactions with critically important biomolecules inside the bacterial cell. In the current study, Fe_3O_4-NPs demonstrated significant antibacterial activity against both *Escheria coli* and *Staphylococcus aureus* strains. Fe_3O_4 showed antibacterial effect against gram-positive as well as gram-negative bacteria which clearly indicates that these nanoparticles are effective antibacterial activity. Table 5 below shows the antibacterial activity of Fe_3O_4 nanoparticles that synthesized by green within different ratio and that of synthesized by chemical method. As compared to the antibacterial activity of green synthesized Fe_3O_4 nanoparticles, S11 is more effective than that of S21 at both gram negative and gram positive bacteria. This can be occurred due to the difference of their size. Although as seen from Table 5 S12 uncalcinated was effective than that of calcinated in gram negative and almost the same on gram positive bacteria and as compared S12 calcinated to S11, S12 is anti bacterial effective than that of S11. This was due to the different active molecules found in the *Hagenia abyssinica* flowers that used in excess amount of extract in S12 than that of S11.

Chemically synthesized Fe_3O_4 nanoparticles were effective than green synthesized Fe_3O_4 nanoparticles. This may occurred due to their shapes. However both, Fe_3O_4 nanoparticles were almost the same effective antibacterial activity on both gram negative and gram positive bacteria. As compared the effective of Fe_3O_4 nanoparticles synthesized by green method and chemical method, almost both of them have same effective on both gram negative and gram positive bacteria. The Fe_3O_4 Nanoparticle showed a good antibacterial activity on *E. coli* and *S. aureus*

bacterial strains. The gram-negative bacteria are more sensitive when compared to gram-positive bacteria.

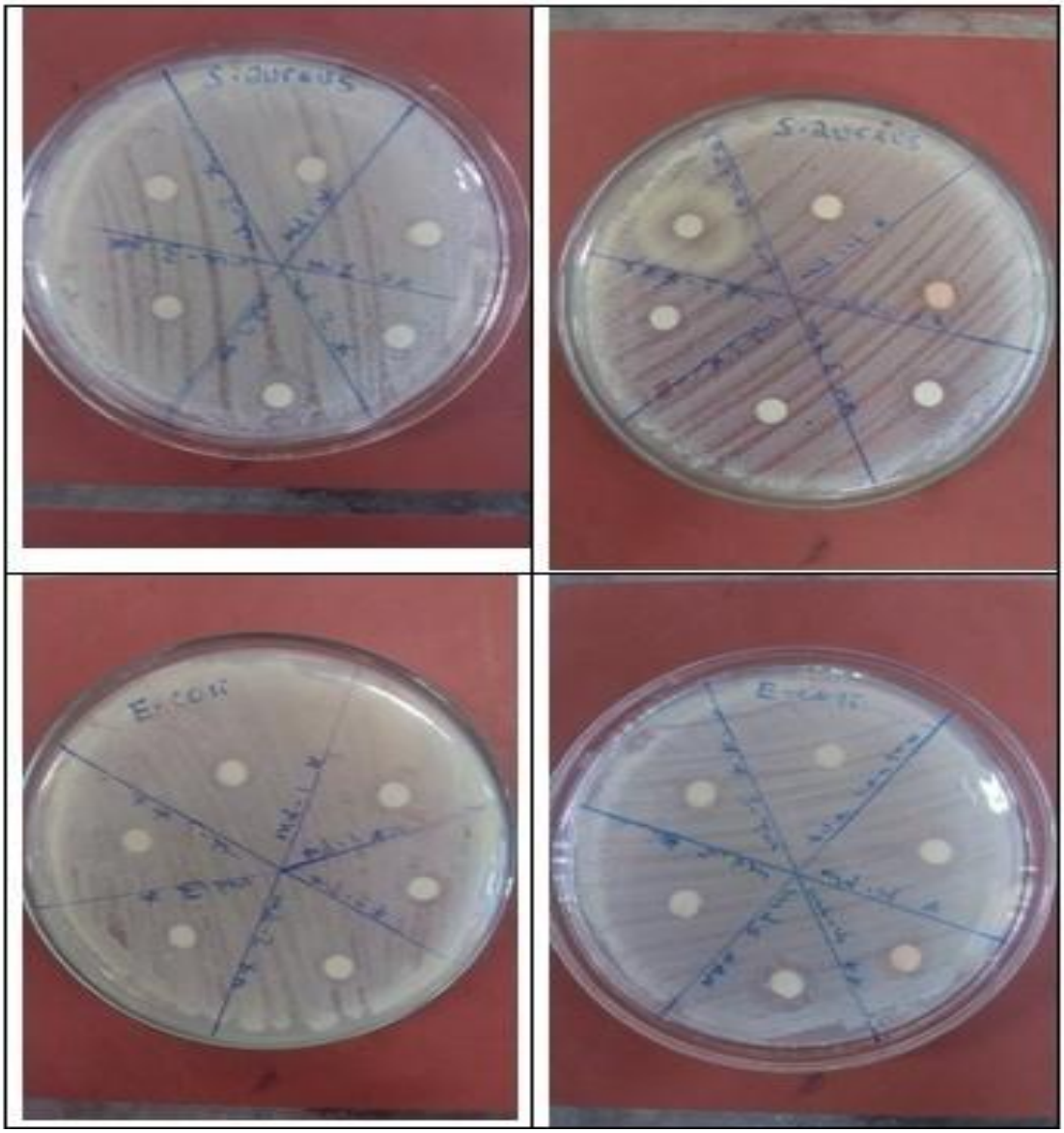

Figure 12: Studies of antibacterial activity (zone of inhibition) of Fe_3O_4 nanoparticles.

Table 5: Antibacterial activity of iron oxide nanoparticles

S.no	Sample name	Zone of inhibition Average (mm)							
		E.coli (Gram negative Bacteria)			Postive control (Ciproflo xacin)	*S.aureus* (Grampositive Bacteria)			Postive control (Ciprofloxa cin)
		Concentration μg /ml				Concentration μg/ml			
		25	50	75	27.33	25	50	75	25.5
1	Fe_3O_4 (2:1)	10	11	12		10.3	12	12.3	
2	Fe_3O_4 (1:2)	11.6	14.3	14.5		10.6	12.3	12.5	
3	Fe_3O_4 (1:2) Calcinated	10	13	13.3		11.3	11.6	13	
4	Fe_3O_4 (1:1)	10.3	12.3	14.6		11	12	13.3	
5	Fe_3O_4(chemically synthesized)	12.5	14	16		11.6	12	14.3	

In the present study, metal oxide (FeO) could be the source that created ROS leading to the inhibition of most of the pathogenic bacteria including *Staphylococcus aureus*. A similar process was also described by (Kim *et al.* 2007). Fe^{2+} reacted with oxygen to create hydrogen peroxide (H_2O_2). In this study the bacteria effect was also based on the particle size of nanoparticles. For example in the case of S11 and S21 the size of sample (S11) smaller than that of sample (S21), So S11 was more effective than S21. Different researcher also report that the small size of nanoparticles can also contribute to the bactericidal effects (Lee *et al*., 2008) .They reported that the inactivation of *Escherichia coli* by zero-valent iron nanoparticles could be

because of the penetration of the small particles (sizes ranging from 10 - 80 nm) into *E. coli* membranes.

In the present study, the concentration of nanoparticles was a major factor for anti- bacterial activity of the nanoparticle. From this study observed that as concentration increase from 25 – 75 µg/ml the antibacterial activity also increase. A similar concentration-dependent behavior was observed by (Kim *et al.,* 2007). Generally in this studies Fe_3O_4 nanoparticles that synthesized by both green method and chemical method shows the effective antibacterial activity on both gram negative and gram positive bacterial strains.

5. CONCLUSION AND RECOMMENDATION

5.1. Conclusion

Green synthesis of iron oxide (Fe_3O_4) nanoparticles using *H. abyssinica* flower extract and chemical synthesis of Fe_3O_4 nanoparticles has been established. Fe_3O_4 nanoparticles were successfully synthesized using ferric chloride hexahydrate and ferrous sulphate hepta hydrate precusor and *H. abyssinica* using flower extract within different ratios and chemical synthesized using ferric nitrate precursor and ethylene glycol. Fe_3O_4 nanoparticles synthesized both using green method and chemical method were characterized by advanced instruments.

In green synthesized of Fe_3O_4 nanoparticles good result was obtained when the ratio of precusor used and plant extract used was equal. When the plant extract was greater than precusor used the crystalline nature of of the particle lost and when the precusor used was greater than that of plant extract, there was high yield of sample and its have good crystalline nature. XRD result indicates that the particles size was found to be from 8- 9.2 nm for green Fe_3O_4 nanoparticles and 9.28 nm for that of chemically synthesized Fe_3O_4 nanoparticles. SEM analysis result indicates flower shape for green synthesized nano samples and rod shape for chemically synthesized nano sample. EDS analysis shows the presence of Fe and O and also presence of few foreign matter. This was occurred during chacterization of SEM from the standard of insrument.nano samples.

UV-Vis result shows the reflectance peak of green Fe_3O_4 nanoparticles at 324.4 nm and that of chemically synthesized Fe_3O_4 nanoparticles at 328.5 nm. FTIR analysis indicates the presence of various capping agents in the flower extract of *H.abyssinica* and also indicates the metal oxide bond formation for both synthesis method of Fe_3O_4 nanoparticles.

In this study the antibacterial activity of green synthesized Fe_3O_4 nanoparticles by different ratios and chemically synthesized Fe_3O_4 nanoparticles was tested on two bacterial strains by using 25, 50 and 75µg/ml concentration to test bacterial activity . i.e on gram negative *E.coli* and gram positive *S.aureus* bacterial strain. The result shows the gram negative bacterial activity was more sensitive than that of gram positive bacterial activity for both chemical and green method. Chemically synthesized Fe_3O_4 nanoparticles was active than that of green synthesized Fe_3O_4 nanoparticles for antibacterial activity. In this studies almost both chemical and green

synthesized Fe_3O_4 nanoparticles were sensitive for antibacterial activity on both bacterial strains. General from this studies observe that the green synthesis method were more useful than chemical method. Because green method was cost effective, non toxic and enviromental friendly.

5.2. Recommendation

Further research is needed to prepare on the other parts of *H. abyssinica* plant such as leaves, stems, roots and etc.

Use NMR spectroscopy to provides the exact molecular structure of the compound obtained from the plants used and also to know the biomolecules found in the plant that used as reducing and capping agent.

Moreover, more experiments should be done with other metal oxide nanoparticles for antibacterial activity on other bacterial strain.

6. REFERENCE

Abou El-Nour, K.M.; Eftaiha, A.; Al. Warthan and A. Ammar., R.A. (2010). Synthesis and applications of silver Nanoparticles, *Arab. J. Chem***.** 3: 135–140.

Aftabtalab, A. and Sadabadi, H. (2015). Application of Magnetite (Fe_3O_4) Nanoparticles in Hexavalent Chromium Adsorption from Aquatic Solutions, *J. Pet Environ Biotechnol* 6:200.

Ahmad, N., Sharma, S., Singh, V.N., Shamsi, S.F., Fatma, A., Mehta, B.R. (2011). Biosynthesis of Silver Nanoparticles from Desmodiumtriflorum: a novel approach towards weed utilization, *Int. Biotech. Res*. 1:8.

Ahmad, S., Farrukh, M. A., Khan, M., Khaleequr-Rahman, M. and Tahir, M. A. (2014). Synthesis of iron oxide–tin oxide nanoparticles and evaluation of their activities against different bacterial strains, *Canadian Chemical Transactions*, 2: 122–133.

Arap W, Pasqualini R., Ruoslahti E. (1998). Cancer treatment by targeted drug delivery to tumor vasculature in a mouse model. *Sci*. 279(5349):377-80.

Arivalagan K, Ravichandran S, Rangasamy K and Karthikeyan E. (2011). Nanomaterials and its potential applications, *Int. J. ChemTech Res*. 3: 534.

Arokiyaraj, S., Saravanan, M., Prakash, N. U., Arasu, M. V., Vijayakumar, B. and Vincent, S. (2013). Enhanced antibacterial activity of iron oxide magnetic nanoparticles treated with Argemone Mexicana L. leaf extract: An in vitro study. *Materials Research Bulletin*, 48(9):3323–3327.

Azam, A., Ahmed, A. S., Oves, M., Khan, M. S., Habib, S. S., & Memic, A. (2012). Antimicrobial activity of metal oxide nanoparticles against gram-positive and gram-negative bacteria: A comparative study. *International Journal of Nanomedicine*, 7: 6003.

Bhosale, R.R.; Kulkarni, A.S.; Gilda, S.S.; Alorkar, N.H.; Osmani, R.A.; Harkare, B.R. (2014). Green Synthesis and Characterization of Iron Oxide Nanoparticles Using Phyllanthus Niruri Extract, *Int. J. Pharm. Sci. Nanotech*, 7: 2330.

Birnbaum A. J. and A. Pique. (2011).“Laser induced extra-planar propulsion for three dimensional micro fabrication, *“Applied Physics Letters*, vol. 98(13): 134101–134106.

Boxall C, Kelsall G and Zhang Z. (1996). Photoelectrophoresis of colloidal iron oxides. Part 2: magnetite (Fe3O4), *J. Chem.Soc. Faraday Trans*. 92: 791

Cao M, Li Z, Wang J, Ge W, Yue T, Li R, Colvin V L and Yu W. (2012). Food related applications of magnetic iron oxide nanoparticles: enzyme immobilization, protein purification, and food analysis Trend. *Food Sci. Technol*, 27: 47.

Chaki, S.H., Malek, T.J., Chaudhary, M.D, Tailor, J.P., Deshpande,M.P. (2015). Magnetite Fe_3O_4 nanoparticles synthesis by wet chemical reduction and their characterization.*Adv. Nat. Sci, Nanosci. Nanotechnol*, 6: 1-7.

Chatzimitakos, T. G. and Stalikas, C. D. (2016). Qualitative alterations of bacterial Metabolome after exposure to metal nanoparticles with bactericidal properties: A comprehensive workflow based on 1H, NMR, UHPLC-HRMS, and metabolic databases. *Journal of Proteome Research*, 15(9): 3322–3330.

Cheng. F, J. W. Betts, S. M. Kelly, J. Schaller, and T. Heinze, (2013). “Synthesis and antibacterial effects of aqueous colloidal solutions of silver nanoparticles using aminocellulose as a combined reducing and capping reagent,” *GreenChemistry*, vol. 15(4): 989 – 998.

Chokriwal, A. (2014). Biological Synthesis of Nanoparticles Using Bacteria and their Applications. *In: American Journal of PharmTech Research*, 4 (6): 38-61.

Chung S, Hoffmann A, Bader S, Liu C, Kay B, Makowski L, Cheng, L. (2004). Biological sensors based on Brownian relaxation of magnetic nanoparticles, *Appl. Phys. Lett*. 85: 2971-2973.

Cornell, R .M and Schwertmann U. (2003). The Iron Oixdes: Structures, Properties, Reactions, and Occurences used (Weinheim: Wiley).

Cornell, R.M and Schwertmann U. (1996). The iron oxides.VCH Press, Weinheim, Germany, pp 573.

Darbandi M, Stromberg F, Landers J, Reckers N, Sanyal B. (2012). Nanoscale size effect on surface spin canting in iron oxide nanoparticles synthesized by the micro emulsion method. *J Phys D: Applied Physics,* 45:195001.

Duan F, Guojun, J. (2005). Introduction to condensed matter physics, *World Scientific, Singapore*, 1: 616.

Eiglesias S., J. Rivas., L. M., Leon, Isidro and M. A., Lopez Quintela. (2007).“Synthesis of Silver Coated Magnetic Nano- particles,” *Journal of Non Crystal Solids*, 353, (8- 10): 829-831.

Estelrich J, Escribano E, Queralt J, Busquets MA. (2015). Iron oxide nanoparticles for magnetically-guided and magnetically-responsive drug delivery. *Int. J. Mol. Sci*. 16(4):8070–8101.

Faller, p., M.A., D.J. Sheehan, J.H. Rex. (2004). Determination of fungicidal activities against yeasts and molds: lessons learned from bactericidal testing and the need for standardization, *Clin. Microbiol. Rev*. 17: 268–280.

Figuerola A, Di Corato R., Manna L., Pellegrino T. (2010). From iron oxide nanoparticles towards advanced iron-based inorganic materials designed for biomedical applications, *Pharmacol, Res*. 62: 126- 143.

Ghandoor H.El, Zidan H. M, Mostafa M.H. Khalil and Ismail M. I. M. .(2012). Synthesis and Some Physical Properties of Magnetite (Fe_3O_4) Nanoparticles, Int. J. Electrochem. Sci., 7: 5734 – 5745.

Glasgow W, Fellows B, Qi B, et al. (2016). Continuous synthesis of iron oxide (Fe_3O_4) Nanoparticles via thermal decomposition, *Particuology,* 26:47-53.

Gordon, T. (2011). Synthesis and characterization of zinc/iron oxide composite, Nanoparticles and their antibacterial properties, *Colloids and Surfaces* A: *Physicochemical and Engineering Aspects*. 374(1): 1-8.

Gupta, A. K.; Gupta, M. (2005) .Synthesis and surface engineering of iron oxide nanoparticles. for biomedical applications, *Biomaterials,* 26: 3995-4021.

Hajipour, M. J.; Fromm, K. M.; Ashkarran, A. A.; Aberasturi, D. J. d.; Larramendi, I. R. d.; Rojo, T.; Serpooshan, V.; Parak, W. J. Mahmoodi., M. (2012). Antibacterial properties of nanoparticles, *Trend. Biotechnol, 30(10):* 499-511.

Hemingway BS. (1990). Thermodynamic properties for bunsenite, NiO, magnetite, Fe_3O_4 and hematite, Fe_2O_3 with comments on selected oxygen buffer reactions. *American Mineralogist* 75: 781-790.

Hill RJ, Craig JR., and Gibbs, GV. (1979). Systematics of the spinel structure type , *Physics* and *Chemistry, of Minerals*, 4:317-339.

Horikoshi S. and N. Serpone, (2014). Microwaves in nanoparticle synthesis*: Fundamentals* and *applications*: John Wiley & Sons, 53:7986.

Hufschmid R, Arami H and Ferguson RM.(2015).Synthesis of phase-pure and monodisperse iron oxide nanoparticles by thermal decomposition, *Nanoscale,* 7(25):11142- 11154.

Hui, C., Shen, C., Yang, T., Bao, L., Tian, J. & Ding, H. (2008). Large-scale Fe_3O_4 nanoparticles soluble in water synthesized by a facile method. *J. Phys. Chem. C* 112(30) : 11336–11339.

Jansen, P. C. M. (1981). Spices, condiments and medicinal plants in Ethiopia, their taxonomy and agricultural significance, 906:194-205.

Jeffrey L., Watts, Rm., Thomas R., Shryock, Michael, Apley, Dvm., Donald J., Bade Steven D., Brown, Jeffrey T., Gray, Henry Heine, Rob P., Hunter, Ms, Dik J., Mevius, Dvm, Mark G., Papich, Dvm., Ms Peter Silley, Gary E. And Zurenko, MS.(2008). Performance Standards for Antimicrobial Disk and Dilution Susceptibility Tests for Bacteria Isolated from animals; *Approved Standard third edition, Clinical and Laboratory Standards Institute*, 28(8).

Jiang, Wu, W.; He, Q.G.; C.Z. (2008). Magnetic iron oxide nanoparticles: Synthesis and surface fictionalizations strategies, *Nanoscale, Res. Lett*. 3: 397–415.

Jing Xu, Haibin Yang, Wuyou Fu, Kai Du, Yongming Sui, Jiuju Chen, Yi Zeng, Minghui Liand Guangtian Zou. (2007). Preparation and magnetic properties of magnetite nanoparticles by sol–gel method, *Journal of Magnetism and Magnetic Materials*, 309: 307–311.

Jiang, C.,Wu, W.Z W.,Yu, T., Kim, W.S., (2015). Recent progress on magnetic iron oxide Nanoparticles. *Sci. Technol. Adv. Mater*. 16 :1-43.

Kandpal, N.D., (2014). Co-precipitation method of synthesis and characterization of iron oxide nanoparticles, *Journal of Scientific & Industrial Research*, 73(2): 87-90.

Khorrami MB, Sadeghnia HR, Pasdar A, Ghayour- Mobarhan M, Riahi-Zanjani B, Darroudi M. (2018). Role of pullulan in preparation of ceria nanoparticles and investigation of their biological activities. *J. Mol Struct.* 1157:127-131.

Kim, J. S., E. Kuk and K. N. Yu. (2007).“Antimicrobial Effects of Silver Nanoparticles,” *Nanomedicine*: *Nanotechnology, Biology and Medicine*, 3 (1): 95 -101.

Kiruba Daniel, S.C.G., Vinothini, G., Subramanian, N., Nehru, K., Sivakumar, M. (2013). Biosynthesis of Cu, ZVI and Ag nanoparticles using Dodonaea viscosa extract for antibacterial activity against human pathogens, *J. Nano Res*, 15(1):1-10.

Kojima K, Miyazaki M, Mizukami F and Maeda K.(1997). Selective formation of spinel iron oxide in thin films by complexing agent-assisted sol-gel processing. *J Sol-Gel Sci Technol*. 8(1–3):77–81.

Kowshik, M.S. Ashtaputre, and S. Kharrazi. (2003).“Extracellular synthesis of silver nanoparticles by a silver-tolerant yeast strain MKY3,” *Nanotechnology*, 14(1): 95–100.

Kumar, Amit, (2012). Phytochemical, ethnobotanical and pharmacological profile of *Lagenaria siceraria*:-A Review. *J. Pharmacog Phytochem*, 1: 27-35.

Kumar, V. G and Ananthu A. Prem. (2018). Green synthesis and characterization of iron oxide nanoparticles using Phyllanthus Niruri extract, *Oriental Journal of Chemistry*, 34 (5): 2583-2589.

Laurent S, Dutz S, Häfeli U O and Mahmoudi M. (2011) Magnetic fluid hyperthermia: focus on superparamagnetic iron oxide nanoparticles, *Adv. Colloid Interface Sci*. 166: 8.

Laurent, S., Forge, D., Port, M., Roch, A., Robic, C., Vander Elst, L. and Muller, R. N. (2008).Magnetic iron oxide nanoparticles: Synthesis, stabilization, vectorization, physicochemical characterizations, and biological applications. *Chemical Reviews*, 108(6): 2064–2110.

Lee. C, J. Y. Kim, W. I. Lee, K. L. Nelson, J. Yoon and D. L. Sedlak, (2008). “Bactericidal Effect of Zero-Valent Iron Nanoparticles on *Escherichia coli*,” *Environmental Science & Technology*, 42(13): 4927-4933.

Lee, N and Hyeon T. (2012). Designed synthesis of uniformly sized iron oxide nanoparticles for efficient magnetic resonance imaging contrast agents *Chem. Soc. Rev*. 41: 2575.

Li, Y., Chen, Z. and Gu , N. (2012). In vitro biological effects of magnetic nanoparticles, *Chinese Science Bulletin*, 57(31): 3972–3978.

Lu A H, Salabas E L and Schuth F. (2007). Magnetic nanoparticles: synthesis, protection, functionalization, and application Angew. *Chem. Int. Edn*. 46:1222.

Manoranjan Arakha, Sweta Pal, Devyani Samantarrai, Tapan K. Panigrahi, Bairagi C. Mallick, Krishna Pramanik2, Bibekanand Mallick1 & Suman Jha, (2015). Antimicrobial activity

of iron oxide nanoparticle upon modulation of nanoparticle bacteria interface, *Scientific Reports,* 5:14813.

Masalha M, Borovok I, Schreiber R, Aharonowizit Y. and Cohen G. (2001). Analysis of transcriptio of the staphylococcus aureus aerobic class Ib and anaerobic class III ribonucleotides reductase genes in response to oxygen, *Journal of Bacteriology,* 183(24) : 7260-7272.

Mittal, A.K., Chisti, Y. and Banerjee, U.C. (2013). Synthesis of Metallic Nanoparticles Using Plant extracts, *In Biotechnology Advances* , 31 (2): 346-356

Mohanpuria, P., N. K. Rana, and S. K. Yadav, (2008).“Biosynthesis of nanoparticles: technological concepts and future applications, *“Journal of Nanoparticle Research*, 10 (3): 507–517.

Negash, L. (1995). Indigenous trees of Ethiopia biology, uses and propagation techniques. 125-148.

Nurbas, M., Ghorbanpoor, H. and Avci, H. (2017). An eco-friendly approach to synthesis and characterization of magnetite (Fe_3O_4) nanoparticles using *platanusorientalis l.* Leaf extract, *Digest Journal of Nanomaterials and Biostructures,* 12(4): 993 - 1000.

Pankhurst QA, Connolly J, Jones SK and Dobson, J. (2003). Applications of magnetic nanoparticles in biomedicine, *Journal of Physics D. Applied Physics*, 36: 167.

Raghunath, A. and Perumal, E. (2017). Metal oxide nanoparticles as antimicrobial agents: A Promise for the Future, in *International journal of antimicrobial agents*, 49(2) : 137-152.

Rahman, O. (2012). Magnetite (Fe_3O_4) nanoparticles for chromium removal .*Mater, Chem. Phys*. 132: 196

Rai, M., Yadav, A., Gade, A. (2008). CRC 675 current trends in phytosynthesis of metal nanoparticles, *Critic*. *Rev*. *Biotechnol*, 28(4): 277–284.

Raja, K.; Verma, S.; Karmakar, S.; Kar, S.; Jerome Das, S.; Bartwal, K.S. (2011). Synthesis and Characterization of Magnetite, Nanocrystals, *Cryst. Res. Technol*. 46:497–500.

Saba Hasan, (2015). A Review on Nanoparticles, Their Synthesis and Types, *Res. J. Recent Sci.* 4: 9-11.

Saqib S, Munis MFH, Zaman W. (2018). Synthesis, characterization and use of iron oxide nanoparticles for antibacterial activity, *Microsc. Res Tech*. 82(4) 1–6.

Sara Shaker, Shirzad Zafarian, CH. Shilpa Chakra and K.Venkateswara Rao. (2013). preparation and characterization of magnetite nanoparticles by sol-gel method for water treatment, *International Journal of Innovative Research in Science, Engineering and Technology*, 2 :7

Sathishkumar G., Logeshwaran V., Sarathbabu S., Pradeep K. Jhac, Jeyaraj M.d, Rajkuberan C.,

Senthilkumar N. and Sivaramakrishnan S. (2018). Green synthesis of magnetic Fe_3O_4 nanoparticles using *Couroupita guianensis Aubl*. fruit extract for their antibacterial and cytotoxicity activities, *Nanomedicine and Biotechnology*, 46(3) : 589-598.

Seil, J. T. and Webster, T. J. (2012). Antimicrobial applications of nanotechnology: Methods and literature, *International Journal of Nanomedicine*, 7: 2767.

Senthil, M, Ramesh, C. (2012). Biogenic synthesis of Fe_3O_4 nanoparticles using Tridaxprocumbens leaf extract and its antibacterial activity on Pseudomonas aeruginosa. *J. Nanomat, Biostruc*. 7: 1655-1660.

Shah. M, D. Fawcett, S. Sharma, S. K. Tripathy, and G. E. J. Poinern, (2015). "Green synthesis of metallic nanoparticles via biological entities," *Materials*, 8 (11): 7278–7308.

Singh, R., Smitha, M.S. & Singh, S.P. (2014).The role of nanotechnology in combating multi-drug resistant bacteria, *J. Nanosci. Nanotechnol*, 14(7): 4745–4756.

Sportelli, M. C., Picca, R. A., & Cioffi, N. (2016). Recent advances in the synthesis and characterization of nano antimicrobials. TrAC Trends, *in Analytical Chemistry*, 84: 131–138.

Srivastava M, Chaubey A, Ojha, AK. (2009). Investigation on size dependent structural and magnetic behavior of nickel ferrite nanoparticles, prepared by sol-gel and hydrothermal methods. *Mater, Chem Phys*. 118(1):174-180.

Sun A., Wu S., Zhai F, J.Wang. (2011). Fe_3O_4 magnetic nanoparticles synthesis from tailings by ultrasonic chemical co-precipitation, *Mat. Lett* .65(12):1882–1884.

Tartaj P, Morales MDP, Veintemillas-Verdaguer S, Gonzalez-CarrenoT, Serna CJ. (2003). The preparation of magnetic nanoparticles for applications in biomedicine. *J. Phys D: Appl Phys.* 36: 182-197.

Teja AS. and Koh, PY. (2009). Synthesis, properties, and applications of magnetic iron oxide nanoparticles, *Progress in Crystal Growth and Characterization of Materials*, 55(1-2):22-45.

Thakkar, K.N., Mhatre, S.S., Parikh, R.Y. (2010). Biological synthesis of metallic nanoparticles, *Nanomedicine*, 6(2): 257–262.

Tran, N., Mir, A., Mallik, D., Sinha, A., Nayar, S., Webster, T.J. (2010). Bactericidal effect of iron oxide nanoparticles on Staphylococcus aureus, *Int .J. Nanomed*, 5(1): 277–283.

Vicky, M., Rodney, S., Ajay, S., Hardik, M. (2010). Introduction to metallic nanoparticles, *J. Pharm. Bioallied Sci.* 2(4): 282-289.

Wang, L., Hu, C. and Shao, L. (2017). The antimicrobial activity of nanoparticles: Present situation and prospects for the future. *International Journal of Nanomedicine*, 12: 1227–1249.

Wei, Wu. Quanguo, He and Changzhong, Jiang. (2008). Magnetic Iron Oxide Nanoparticles: Synthesis and Surface Functionalization Strategies, *Nano Review*, 3:397–415.

Wool house, M., Ward, M., van Bunnik, B. and Farrar, J. (2015). Antimicrobial resistance in humans, livestock and the wider environment, *Philosophical Transactions of the Royal Society B.* 370(1670) : 1471-2970

Wu W, He, Q and Jiang C. (2009). Magnetic iron oxide nanoparticles: synthesis and surface functionalization strategies. *Chem.Inform*. 40(24): 1.

Wu W, Xiao X H, Zhang S F, Zhou J A, Fan L X, Ren F and Jiang C Z. (2010). Large-scale and controlled synthesis of iron oxide magnetic short nanotubes: shape evolution, growth mechanism, and magnetic properties *J. Phys.Chem. C*. 114:16092.

Xu, Y., Wei, M.-T., Ou-Yang, H. D., Walker, S. G., Wang, H. Z., Gordon, C. R., Brink, P. R. (2016). Exposure to TiO_2 nanoparticles increases Staphylococcus aureus infection of Hela cells. *Journal of Nanobiotechnology*, 14(1): 34.

Yamamoto, O. (2001). Influence of particle size on the antibacterial activity of zinc oxide. *Int J. Inorg. Mater*, 3(7): 643–646.

Yang L. (2008). Development of receptor targeted magnetic iron oxide nanoparticles for efficient drug delivery and tumor imaging, *J. Biomed. Nanotechnol*, 4: 439.

Yetter, AR. Risha, GA. and Son, SA . (2009). Metal particle combustion and nanotechonology, *P .Combust Inst.* 32(2):1819-1838.

Yuvakkumar, R and Hong, SI. (2014). Green synthesis of spinel magnetite iron oxide nanoparticles, *Adv Mater Res*. 1051 : 39–42.

Zhang Z, Boxall C and Kelsall G H. (1993). Photoelectrophoresis of colloidal iron oxides: 1. Hematite (α-Fe_2O_3). *Colloids Surf.*73:145-163.

APPENDIX

Appendix 3: XRD Spectrum of green uncalcinated synthesized Fe_3O_4 nanoparticle

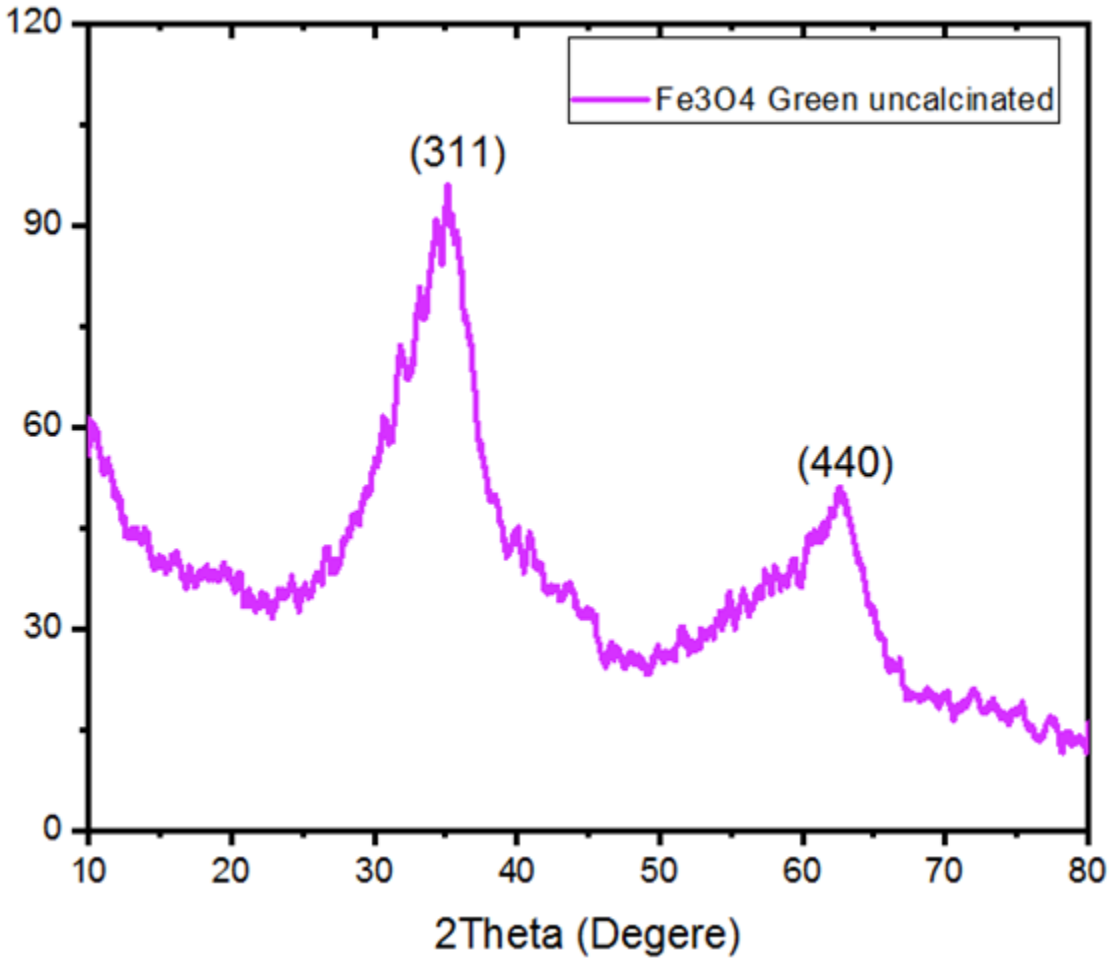

.

Appendix 4: XRD Spectrum of chemical uncalcinated synthesized Fe_3O_4 nanoparticles.